Identification of a Novel Orally Bioavailable ERK5 Inhibitor with Selectivity over p38α and BRD4.

*Stephanie Myers,[a◊] Duncan C. Miller,[a◊] Lauren Molyneux,[a◊] Mercedes Arasta,[b] Ruth H. Bawn,[a] Timothy Blackburn,[a] Simon J. Cook,[c] Noel Edwards,[b] Jane A. Endicott,[b] Bernard T. Golding,[a] Roger J. Griffin,[a♱] Tim Hammonds,[d] Ian R. Hardcastle,[a] Suzannah J. Harnor,[a] Amy Heptinstall,[a] Pamela Lochhead,[c] Mathew P. Martin,[b] Nick C. Martin,[a] David R. Newell,[b] Paul J. Owen,[d] Leon C. Pang,[d] Tristan Reuillon,[a] Laurent J. M. Rigoreau,[e] Huw Thomas,[b] Julie A. Tucker,[b] Lan-Zhen Wang,[b] Ai-Ching Wong,[d] Martin E. M. Noble,[b†] Stephen R. Wedge[b†] and Celine Cano[a†]**

a. Newcastle Drug Discovery, Northern Institute for Cancer Research, School of Chemistry, Bedson Building, Newcastle University, Newcastle upon Tyne, NE1 7RU, UK.

b. Newcastle Drug Discovery, Northern Institute for Cancer Research, Paul O'Gorman Building, Medical School, Framlington Place, Newcastle upon Tyne, NE2 4HH, UK.

c. Signalling Laboratory, The Babraham Institute, Babraham Research Campus, Cambridge, CB22 3AT, UK

d. Cancer Research UK Therapeutic Discovery Laboratories, London Bioscience Innovation Centre, 2 Royal College Street, London NW1 0NH, UK.

e. Cancer Research UK Therapeutic Discovery Laboratories, Jonas Webb Building, Babraham Campus, Babraham, Cambridgeshire CB22 3AT, UK

◊ These authors contributed equally to the work.

† To whom enquiries should be addressed. For enquiries concerning chemistry, contact C.C. Tel (44) 191 208 7060. E-mail: celine.cano@ncl.ac.uk; for enquiries concerning structural biology, contact M.E.M.N. Tel. (44) 191 208 4422. E-mail: martin.noble@ncl.ac.uk; for enquiries concerning bioscience, contact S.R.W. Tel. (44) 191 208 4418. E-mail: steve.wedge@ncl.ac.uk.

✞Deceased 24 September 2014

ABSTRACT

Extracellular regulated kinase 5 (ERK5) signalling has been implicated in driving a number of cellular phenotypes including endothelial cell angiogenesis and tumour cell motility. Novel ERK5 inhibitors were identified using high throughput screening, with a series of pyrrole-2-carboxamides substituted at the 4-position with an aroyl group being found to exhibit IC_{50} values in the micromolar range, but having no selectivity against p38α MAP kinase. Truncation of the *N*-substituent marginally enhanced potency (~ 3-fold) against ERK5, but importantly attenuated inhibition of p38α. Systematic variation of the substituents on the aroyl group led to the selective inhibitor 4-(2-bromo-6-fluorobenzoyl)-*N*-(pyridin-3-yl)-1*H*-pyrrole-2-carboxamide (IC_{50} 0.82 μM for ERK5; IC_{50} >120 μM for p38α). The crystal structure (PDB 5O7I) of this compound in complex with ERK5 has been solved. This compound was orally bioavailable and inhibited bFGF-driven Matrigel plug angiogenesis and tumour xenograft growth. The selective ERK5 inhibitor described herein provides a lead for further development into a tool compound for more extensive studies seeking to examine the role of ERK5 signalling in cancer and other diseases.

KEYWORDS

ERK5; Extracellular regulated kinase 5; BMK1; kinase; bioavailable; pyrrole carboxamide

HIGHLIGHTS

- A sub-micromolar ERK5 inhibitor with selectivity over p38α and BRD4 was developed.
- The binding mode was confirmed by X-ray crystallography.
- *In vitro* and *in vivo* pharmacokinetics confirmed the inhibitor was orally bioavailable.
- The inhibitor suppressed tumour xenograft growth and bFGF-driven Matrigel plug angiogenesis.

INTRODUCTION

Extracellular regulated kinase 5 (ERK5, BMK1, MAPK7) is the terminal kinase in one of the four major mitogen activated protein (MAP) kinase pathways [1]. MAP kinase pathways are central to cancer, as well as numerous other pathologies, and recent clinical success with B-RAF and MEK1/2 inhibitors, in melanoma in particular, has demonstrated that these kinases are amenable to therapeutic exploitation [2]. Correlative clinical data have implicated ERK5 as a potential target in a number of tumour types, including prostate and breast cancer, and mechanistic studies have demonstrated potential roles for ERK5 in cell migration and angiogenesis [3, 4]. Targeting the non-canonical MAPK pathway through inhibition of ERK5 has generated a lot of interest in the last decade. The oxindole-based BIX02189 (Figure 1; **1**) was one of the first potent dual ERK5-MEK5 inhibitors reported [5]. Subsequently, pre-clinical data generated with a pyrimidodiazepinone small molecule inhibitor of ERK5 kinase activity (**2**; XMD8-92) suggested that perturbation of this signalling pathway can impede the growth of human tumours *in vivo* [6].

A more potent and selective ERK5 inhibitor from the pyrimidodiazepinone series, (**3**; AX15836) was subsequently disclosed as a useful tool for the study of ERK5 inhibition [7]. Recently, BAY-885 (**4**) was reported as a potent ERK5 chemical probe [8].

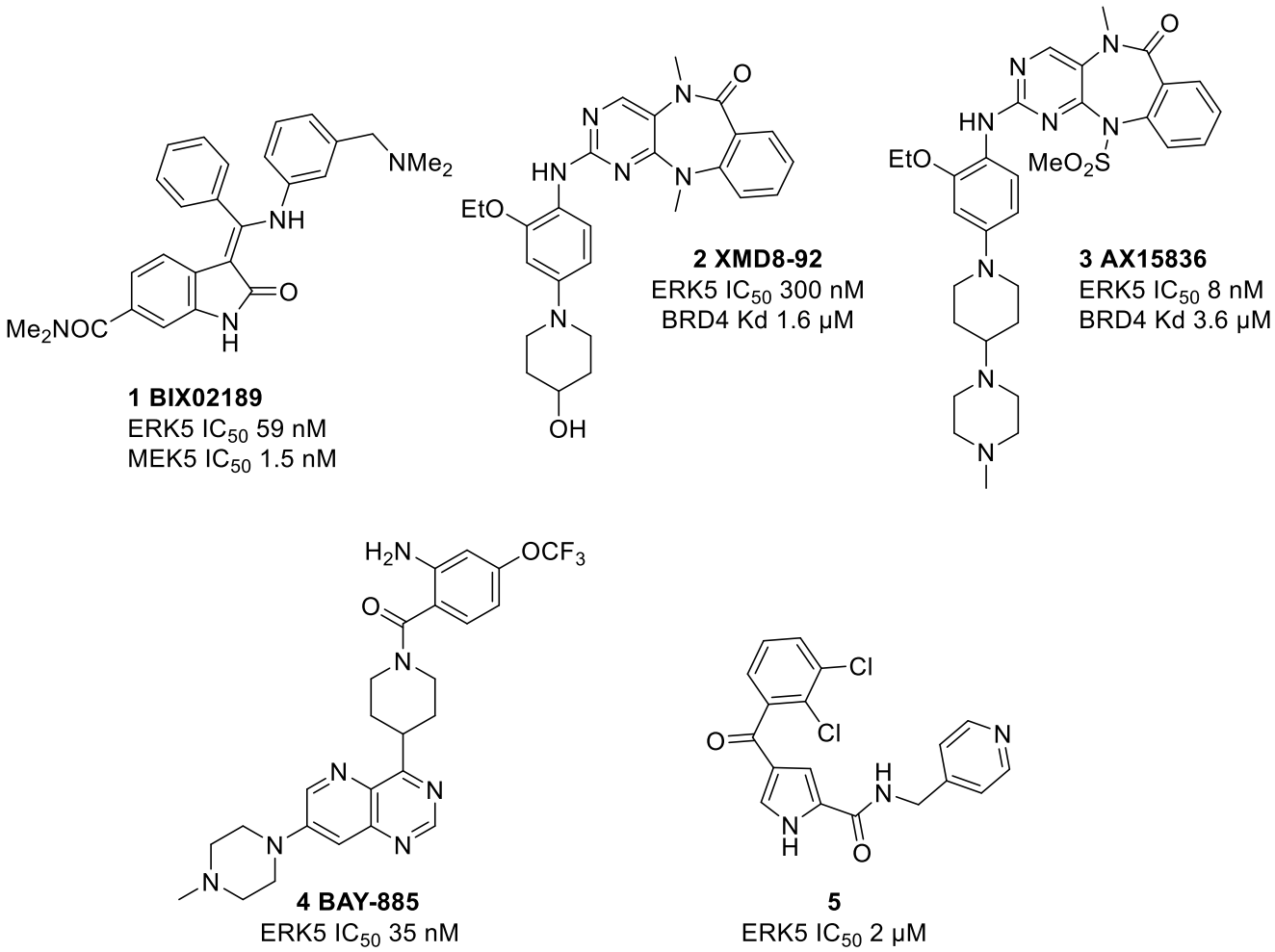

Figure 1. Structures and pharmacological profiles of reported ERK5 inhibitors.

A role for ERK5 in cell proliferation was first indicated by studies using dominant-negative ERK5 constructs that inhibited epidermal growth factor-stimulated proliferation of HeLa cells [9]. However, more extensive recent studies [10], using both MEK5/ERK5 inhibition and ERK5 knockdown, do not support a role for ERK5 in cellular proliferation. In contrast, there are compelling data from a number of studies [11-16] demonstrating that ERK5 signalling promotes

tumour cell migration and invasion, a property that is consistent with the clinical relationship between tumour ERK5 over-expression and metastatic disease. For example, in an orthotopic model of prostate cancer, Leung and colleagues [17] demonstrated that ERK5 promotes the formation of metastases. Similarly, in an *in vivo* orthotopic breast cancer model, ERK5 knockdown resulted in a marked reduction in lymph node metastasis [18].

A third aspect of tumour biology that may be exploited by ERK5 inhibitors is inhibition of tumour angiogenesis. A substantial body of data based initially on constitutive and conditional knockout mouse models shows that ERK5 is required for endothelial cell survival, in particular maintenance of vascular integrity and endothelial cell migration. MEK5, the obligate kinase required for ERK5 activation, and ERK5 knockout mouse embryos die at approximately day 10.5 from tissue failure that includes impaired cardiac development, which may result from an inability to permit maturation of the supporting vasculature [19, 20]. Importantly, in a conditional ERK5 knockout adult mouse model, ERK5 depletion following Cre recombinase induction disrupts vascular integrity and results in death from multiple organ haemorrhage within two to four weeks [21], consistent with a key role for ERK5 in endothelial cell biology [22]. Further studies by Hayashi and colleagues [23] unequivocally link ERK5 signalling to tumour angiogenesis in two *in vivo* mouse tumour models, and in a growth-factor induced angiogenesis model. Consequently, treatment with an ERK5 inhibitor may be anticipated to have a therapeutic effect on tumour vasculature in solid cancers.

Whilst the prototype ERK5 kinase inhibitor, XMD8-92 (**2**) [6], has been used to explore inhibition of ERK5 signalling *in vivo*, a recent study [24] has demonstrated that XMD8-92 (**2**), in common with some other kinase inhibitors [25], can also inhibit bromodomain (BRD) proteins, and that this property may underlie some of the cellular effects of the compound.

Following a high-throughput screening campaign a pyrrole series of ERK5 inhibitors was identified, as exemplified by **5** [26]. Encouragingly, compound **5** passed pan-assay interference (PAINS) and aggregator potential assessment [27]. The current paper describes the hit-to-lead development of potent ERK5 inhibitors in this pyrrole series.

CHEMISTRY

Structure-activity relationships (SARs) were developed for the ketone and amide substituents of lead compound **5**. Regioselective Friedel-Crafts acylation of commercially available methyl pyrrole 2-carboxylate (**6**) using the appropriate acid chloride and aluminium trichloride gave methyl esters **7-18** (Scheme 1).

Hydrolysis of esters **7-18** provided carboxylic acids **19-30**, and subsequent amide coupling mediated by either CDI or PCl_3 furnished inhibitors **31-46**. The PCl_3-mediated coupling conditions proved beneficial with electron-poor amines, where CDI coupling was generally unsuccessful.

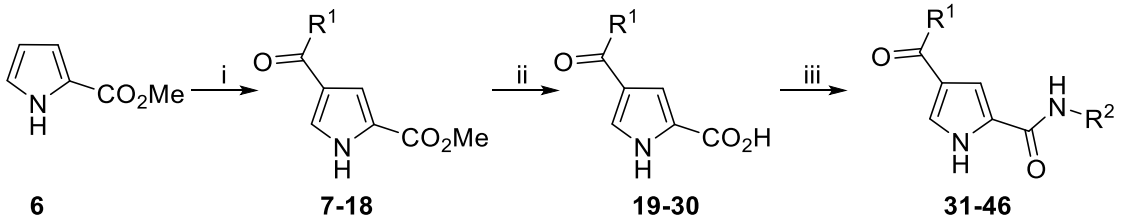

Scheme 1. *Reagents and conditions;* (i) $AlCl_3$, appropriate acid chloride, DCM, 0 °C-RT, 16 h, 22-82%; (ii) LiOH, THF/H_2O, 60 °C, 16 h, 40-99%; (iii) CDI, THF, 70 °C, 3 h; appropriate amine, 50 °C, 3 h then RT, 16 h, 35-95%, or PCl_3, appropriate amine, MeCN, 150 °C, MW, 5-30 min, 48-76%; R groups are defined in Tables 1 and 2.

RESULTS AND DISCUSSION

Following successful hit validation [26], attention initially focussed on developing SARs for substitution of the aroyl ring of **5** in an attempt to improve potency against ERK5, while retaining the most potent 4-picolylamide substituent identified in the initial hit validation campaign [26]. Fluoro substitution at the 2-position (**32**) was beneficial, as was chloro substitution at the 2- or 3-positions (**35**, **36**). Substitution at the 4-position (**34**, **37**) led to loss of ERK5 inhibition. 2,3- or 2,6-disubstitution (**38, 40**) conferred a modest further improvement in potency.

Due to the similarity between published p38α MAP kinase inhibitors [28] and our hit series, a counter-screen against p38α was employed to determine the selectivity of the series. Compounds were generally inversely selective for p38α, with the exception of **40** which showed modest 4-fold selectivity for ERK5.

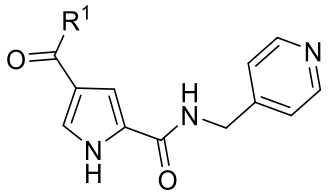

Table 1. Biological evaluation of compounds **31-40**.

ID	R^1	ERK5; IC_{50} (μM)[a]	p38α; IC_{50} (μM)[b]
31	Ph	40 ± 2.6	-
32	2-F-phenyl	5.9 ± 5.9	0.36 ± 0.14
33	3-F-phenyl	>120	-
34	4-F-phenyl	>120	-

35	2-Cl-phenyl	15 ± 2.8	-
36	3-Cl-phenyl	6.3 ± 0.1	6.5 ± 1.9
37	4-Cl-phenyl	>120	-
38	2,3-diF-phenyl	7.0 ± 2.5	2.4 ± 0.75
39	2,6-diF-phenyl	30 ± 32	0.58 ± 0.27
40	2,6-diCl-phenyl	4.4 ± 2.1	12.3 ± 4.7

[a] ERK5 IC_{50}s determined using an IMAP FP Progressive Binding System kit (Molecular Devices #R8127). [b] p38α IC_{50}s determined against full length p38 protein (Millipore #14-251) in a LANCE assay format using a Ulight-MBP peptide substrate. Determinations ± standard deviation (mean of $n \geq 4$).

Attention turned to the amide substituent. Truncated amide groups, lacking the methylene spacer, were synthesised with the aim of improving potency against ERK5 (Table 2). 4-Pyridylamide (**41**) was around 30-fold more potent than its methylene spaced analogue (**39**), exhibiting sub-micromolar ERK5 inhibition. Gratifyingly, truncation of the amide substituent led to a considerable improvement in selectivity over p38α. The 3-pyridylamine regioisomer (**42**) maintained similar ERK5 potency and selectivity. Replacing one of the fluoro substituents with a larger halogen atom, while retaining the second fluoro substituent proved beneficial in terms of both potency and selectivity (**43**-**46**). Five compounds from this series were tested in a cell-based ERK5-dependent MEF2D reporter gene assay. Cellular potency was within 5- to 10-fold of the cell-free IC_{50} values (Table 2), with compounds **43**, **45** and **46** having similar profiles. Due to its

sub-micromolar potency, high selectivity for ERK5 over p38α in cell-free assays, and less than 4-fold difference beween isolated enzyme and cell-free assays, compound **46** was selected as a representative of the pyrrole carboxmide series for further profiling. Growth inhibition in PC3 cells was assessed for compound **46**, which exhibited a GI_{50} of 44 ± 2.8 μM.

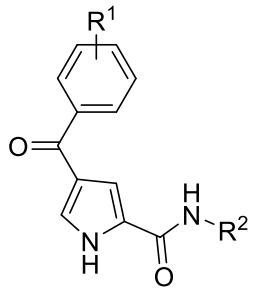

Table 2. Biological Evaluation of compounds **41-46**.

ID	R^1	R^2	ERK5; IC_{50}[a] (μM)	p38α; IC_{50}[b] (μM)	ERK5 MEF2D; IC_{50}[c] (μM)[c]
41	2,6-diF		0.90 ± 0.15	100 ± 35	8.0 ± 10
42	2,6-diF		1.1 ± 0.27	35 ± 0.90	n.d.
43	2-Cl, 6-F		0.60 ± 0.30	>120	2.3 ± 1.5
44	2-Cl, 6-F		0.60 ± 0.20	93.2 ± 12.5	4.0 ± 1.4
45	2-Br, 6-F		0.70 ± 0.20	>120	4.0 ± 2.8
46	2-Br, 6-F		0.82 ± 0.10	>120	3.0 ± 1.2

[a] ERK5 IC_{50}s determined using an IMAP FP Progressive Binding System kit (Molecular Devices #R8127). [b] p38α IC_{50}s determined against full length p38 protein (Millipore #14-251) in a LANCE

assay format using a Ulight-MBP peptide substrate. Determinations ± standard deviation (mean of n ≥ 4). [c] Cell-based activity against ERK5 was determined using a transcriptional reporter assay in which mutationally activated MEK5 (MEK5D) and ERK5 were co-expressed in HEK293 cells and the transactivation domain of the transcription factor MEF2D (an ERK5 substrate) fused to the DNA binding domain of the yeast GAL4 protein. ERK5-dependent activity of GAL4-MEF2D was assayed using a co-expressed luciferase reporter. Determinations ± standard deviation (mean of n = 2).

A crystal structure of the kinase domain of ERK5 in complex with **46** was determined at 2.4 Å resolution, revealing the binding mode for the pyrrole series and rationalising the SAR results (Figure 2, PDB ID 5O7I). As expected, **46** binds in the ERK5 ATP-binding site. The pyrrole *NH* and amide carbonyl form hydrogen bonds with the backbone carbonyl of Asp138 and amide of Met140 from the ERK5 hinge-region, respectively. The 3-pyridinyl substituent lies toward the mouth of the ATP-binding pocket, and is twisted 35° out-of-plane with respect to the amide. Electron density for the pyridyl ring is less well defined than that for the 4-(2-bromo-6-fluorobenzoyl)-1*H*-pyrrole-2-carboxamide moiety, suggesting a degree of rotational freedom about the *N*-*C* bond. The ketone carbonyl lies in plane with the pyrrole ring, and is oriented toward the back of the ATP-binding pocket where it makes a water-mediated hydrogen bond to the backbone amide of Phe201. The 2-bromo-6-fluorophenyl moiety lies in an orthogonal plane to the pyrrole ring, and occupies a hydrophobic pocket formed by the aliphatic portions of the side-chains of Tyr66, Val69, Lys84, Ile115, Leu137, Leu189 and Asp200. This pocket is highly complementary in shape to the 2-bromo-6-fluorophenyl moiety, whilst the orthogonal bioactive conformation is favoured by *ortho*-substitution, accounting for the observed SAR around the aroyl

ring. The side-chain of Tyr66 from the tip of the glycine-rich P-loop that covers the ATP-binding site re-orients to stack edge-to-face against the phenyl ring, explaining the loss of potency for 4-substituted compounds, **34** and **37**.

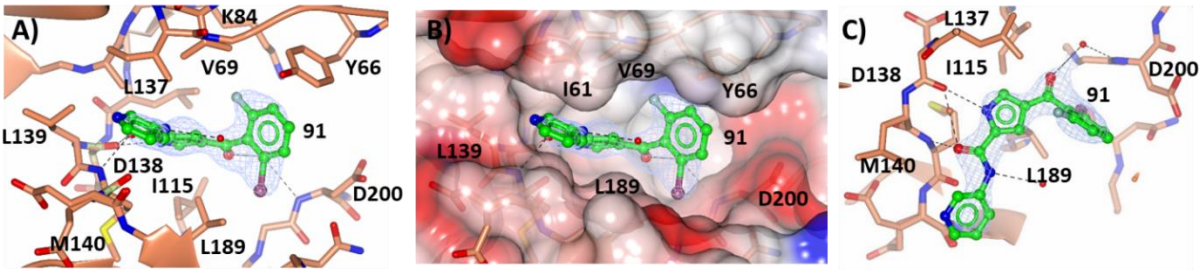

Figure 2. Compound **46** bound at the ERK5 ATP-binding site (PDB ID 5O7I). (a) Crystal structure of the ERK5-**46** complex determined at 2.4 Å resolution, shown in coral ribbon with key active-site residues labelled and shown as sticks, and **46** with carbon atoms in green. The 2Fo-Fc omit electron density, contoured at 1.5 σ around **46**, is displayed as a blue mesh. (b) As (a) with a transparent electrostatic surface drawn over the protein atoms. (c) Top down view of **46** bound within the ERK5 ATP-binding site highlighting the potential hydrogen bonding network formed with the hinge region (D138-M140), and the potential water mediated hydrogen bond formed with D200 of the DFG.

Compopund **46** progressed into further pharmacokinetic and pharmacological profiling. In both human and mouse microsomal stability assays **46** exhibited low intrinsic clearance (HLM Cl_{int} <5 μL/min/mg protein; MLM Cl_{int} 26 μL/min/mg protein) and had high flux and a low efflux ratio (ER) in a caco-2 cell permeability assay (BA >10 × 10^{-6} cm/s, ER 0.82). Solubility, as assessed in a turbidometric solubility assay (Cyprotex), estimated the precipitation concentration of **46** to be >100 μM, (Table 3). **46** had moderate plasma protein binding (F_u 0.06). Compound **46** had an IC_{50} of >5 μM against a panel comprising four cytochrome P450 isoforms (2C19, 2C9, 2D6, 3A4).

When screened at a concentration of 10 μM against a panel of 456 kinases (DiscoverX), in addition to ERK5, **46** inhibited only seven other kinases by ≥ 90% (DCAMKL3, JAK1, SLK, MAP3K15, TYK2, JAK2, MST2 and DCAMKL1; full kinome panel inhibition data can be found in the supplementary information). Overall, **46** showed good drug-like properties and was progressed into *in vivo* drug metabolism pharmacokinetic (DMPK) studies in mice.

A 10 mg/kg dose of **46** was administered through both oral and intravenous routes to female CD1 mice at 8-10 weeks of age (3 mice per time point). The plasma of these mice was collected at eight time points following administration (Table 3). The terminal plasma half-life was 38 min, with a plasma clearance of 27 mL/min/kg, and oral bioavailability of 68%.

Table 3. *In vivo* pharmacokinetic parameters for **46** dosed in female CD1 mice (Charles River, Kent UK) 10 mg/kg either i.v. or p.o.

Administration	**PO**	**IV**
Dose (mg/kg)	10	10
AUC (μg/mL.min)	254	372
$\mathbf{C_{max}}$ (μM)	6	25
$\mathbf{V_d}$ (L/kg)	-	1.2
$\mathbf{T_{max}}$ (min)	15	-
$\mathbf{Cl_p}$ (mL/min/kg)	-	27
$\mathbf{t_{1/2}}$ (min)		38

F (%)	68	-

In vivo efficacy was assessed using a Matrigel plug assay in female CD1 mice (8-10 weeks old) and an A2780 human ovarian carcinoma xenograft model in female CD1 nude (*nu*/*nu*) mice (8-10 weeks old). In both studies, the efficacy of **46** was compared to that of the most advanced ERK5 literature ERK5 inhibitor at the time, XMD8-92 (**2**). The Matrigel plug assay is a measure of angiogenesis and was performed by subcutaneously inoculating mice with 500 μL of Matrigel containing basic fibroblast growth factor (bFGF; 500 ng/mL). This induces formation of a Matrigel plug, which can be permeated by host cells and leads to formation of new blood vessels. In the presence of an anti-angiogenic agent the extent of new blood vessels formed would be reduced. Mice were randomised 24 h following Matrigel inoculation, to receive either; vehicle, XMD8-92 (**2**) (50 mg/kg, i.p.) or **46** (100 mg/kg, p.o.) twice-daily for 7 days (5 mice per group). On day 7 the mice were humanely sacrificed and the Matrigel plugs removed and snap frozen in liquid nitrogen. The concentration of haemoglobin present could then be determined as a surrogate measure for the extent of blood vessel formation. An anti-angiogenic effect was apparent with Matrigel plugs from animals treated with both, XMD8-92 (**2**) (two tailed unpaired *t*-test, $n = 5$, $p = 0.042$) and compound **46** (two tailed unpaired t test $n = 5$ $p = 0.0009$) having lower concentrations of haemoglobin than those from control animals receiving vehicle (Figure 3). There was no significant difference between the two treatments (two tailed unpaired *t*-test, $n = 5$, $p = 0.367$).

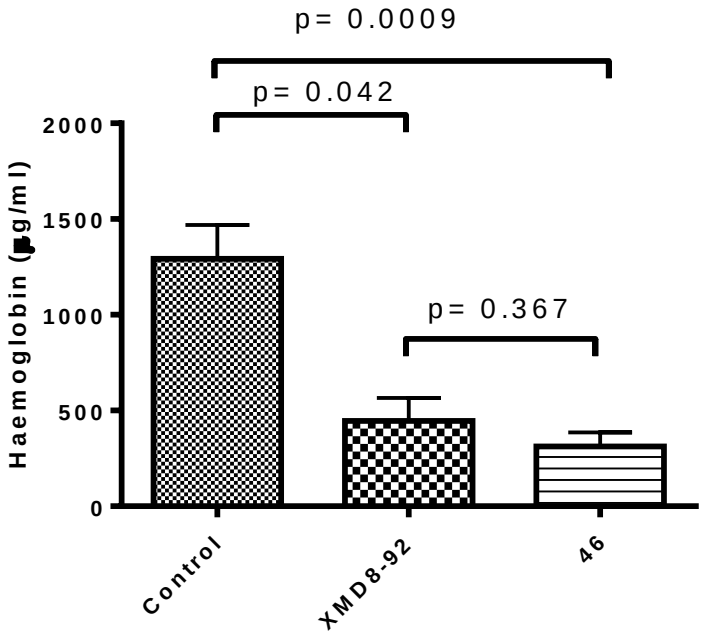

Figure 3. Haemoglobin levels determined in a bFGF Matrigel plug assay. Female CD1 mice, 5 per group, were treated with XMD8-92 (**2**) (50 mg/kg, i.p.) or **46** (100 mg/kg, p.o.) twice-daily for 7 days and *p* values determined using an unpaired two-tailed *t*-test.

In a human tumour xenograft model, mice were inoculated subcutaneously on the right flank with 1×10^7 A2780 human ovarian carcinoma cells, and tumours left to grow for 7 days. The mice (9 per group) were then randomised to receive either vehicle, XMD8-92 (**2**) (50 mg/kg, i.p.) or **46** (100 mg/kg, p.o.) twice-daily for 10 days. Tumour volumes were significantly reduced (as assessed by an unpaired two-tailed *t*-test) in mice treated with either XMD8-92 (**2**) (62% inhibition; p = 0.001) or with **46** (57% inhibition; p = 0.002) when compared to the control group (Figure 4a). Nadir weight was used as an indicator of drug toxicity. None of the animals lost more than 4% of their starting body weight with the nadir body weights being 96% for control, 98% for XMD8-92-treated and 99% for animals in the **46** treatment group (9 mice per group) (Figure 4b). These initial

in vivo studies suggest that an ERK5 inhibitor could have potential as an anti-angiogenic agent and thereby constrain solid tumour growth.

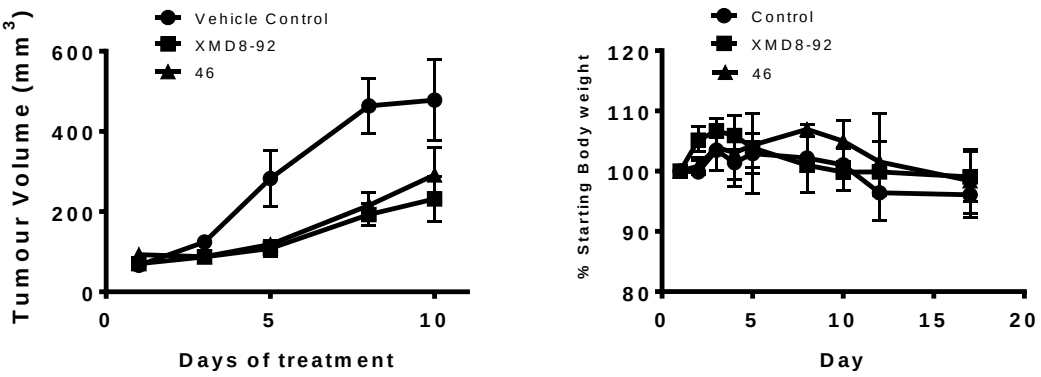

Figure 4. a). Treatment of female CD1 nude mice bearing A2780 human ovarian carcinoma xenografts with vehicle control, XMD8-92 (**2**) (50 mg/kg, ip) or **46** (100 mg/kg, po) (9 per group). Mice were treated twice-daily for 10 days at the end of treatment mean tumour volumes were significantly smaller in mice treated with either XMD8-92 (**2**) ($p = 0.001$) or with **46** ($p = 0.002$) when compared to the control group (unpaired two-tailed *t*-test) b). Percent body weight change over the course of the study.

During the course of the study, we became aware of the recently reported activity of the selective ERK5 inhibitor XMD8-92 (**2**) towards BRD4.[24] Thus, the potential of **46** to interact with the first bromodomain of BRD4 was assessed using Surface Plasmon Resonance (SPR). In contrast to the positive control XMD8-92 (**2**), no binding was observed from the sensorgram for compound **46** (Figure 5), confirming that effects seen in the *in vivo* efficacy models were not due to inhibition of BRD4.

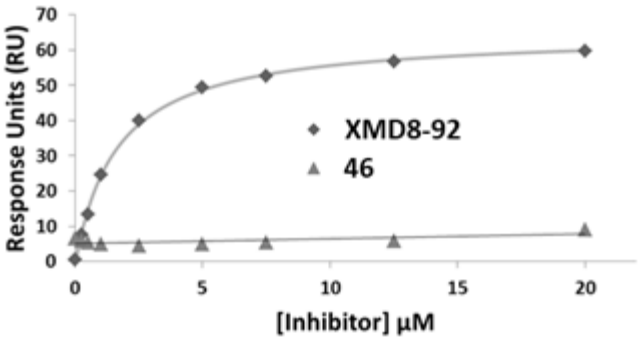

Figure 5. Characterisation of the binding of **46** and XMD8-92 (**2**) to BRD4 by SPR. 1:1 steady-state binding model of **2** and **46** against BRD4, resulting in a K_d of 1.64 µM and no binding, respectively.

CONCLUSIONS

An ERK5 inhibitor with sub-micromolar potency in a cell-free assay has been developed based on a pyrrole carboxamide scaffold through structure-based optimisation of the aryl ketone and amide substituents. Greater than one-hundred fold selectivity over p38α MAP kinase was attained through truncation of the amide substituent. Compound **46** does not interact with the BRD4 bromodomain. Compound **46** exhibited suitable pharmacokinetics in mouse to permit *in vivo* studies following oral dosing and does not interact with the BRD4 bromodomain. Compound **46** suppressed both tumour xenograft growth and bFGF-driven Matrigel plug angiogenesis. Further development of the pyrrole carboxamide series of ERK5 inhibitors to provide compounds with single digit nanomolar ERK5 inhibition in the cell-free ERK5 assay, and sub-micromolar activity in cell-based assays will be the subject of a future publication [29].

EXPERIMENTAL METHODS

Biological Assay Protocols

ERK5 protein production

Cloning of ERK5. The cDNA encoding the catalytic domain of human ERK5 (2-409aa) (NCBI Accession No. BC009963) was cloned into pFastBac-HTb (Invitrogen), which contains an N-terminal 6 x His tag and a TEV cleavage site.

Cloning of ΔN11MEK5DD. Constitutively active mutant form of human MEK5 (NCBI Accession No. BC008838) (MEK5DD) was generated by PCR-based site-directed mutagenesis (QuikChange ® II Site-Directed Mutagenesis kit, Stratagene). The dual phosphorylation sites, serine 311 and threonine 315, were replaced with aspartic acid. Truncated MEK5DD lacking the N-terminal 11 residues (13-448 aa), termed ΔN11MEK5DD, was cloned into pFastBacGST (a modified pFastbac-1 vector that encodes an N-terminal GST tag and a thrombin cleavage site, created in-house).

Baculovirus Production and Protein Expression. *Cell Culture:* Sf9 suspension cultures grown in serum free SF900II medium (Invitrogen) were maintained in shaker flasks at 28 °C with continuous shaking at 150 rpm.

GST-ΔN11MEK5DD and ERK5 recombinant baculoviruses were generated utilizing the Bac-to-Bac baculovirus expression system, as suggested by the manufacturer (Invitrogen).

ERK5 protein was co-expressed with GST-ΔN11MEK5DD by co-infecting Sf9 cells, seeded at a density of $1x10^6$ cells/mL, with both ERK5 and GST-ΔN11MEK5DD viruses at MOIs of 5. 72 h

after infection, the cells were harvested by centrifugation at 1500 rpm for 10 min. The cell pellet was washed with ice-cold PBS and the cells centrifuged as above. The cell pellet was flash frozen in liquid nitrogen and stored at -80 °C until processing.

Protein Purification. 500 mL of harvested SF9 culture lysed by resuspending in 10 mL lysis buffer (50 mM HEPES pH 7.87, 150 mM NaCl, 1% Triton X-100, 50 mM imidazole, 1 mini EDTA-free complete protease inhibitor tablet (Roche), 1% phosphatase inhibitor cocktail 2 (Sigma)) and rolling at 4 °C for 45 minutes. Insoluble material removed by centrifugation and clarified supernatant applied to a 1 mL HisTrap HP column (GE) pre-equilibrated in Buffer A (50 mM HEPES pH 7.87, 150 mM NaCl, 50 mM imidazole). Column washed with 10 CV's Buffer A. Bound protein eluted with a 20 CV linear gradient from Buffer A to Buffer B (50 mM HEPES pH 7.87, 150 mM NaCl, 1 M imidazole); all steps run at 0.5 mL/min.

Fractions containing ERK5/MEK dialysed overnight against Buffer C (50 mM HEPES pH 7.87, 150 mM NaCl) using slidealyzer dialysis membrane, at 4 °C.

Dialysed protein loaded onto a 1 mL CaptoQ trap column (GE), washed with 10 CV's of Buffer C. Bound protein eluted using an 80 CV linear gradient from Buffer C to Buffer D (50 mM HEPES pH 7.87, 1 M NaCl), All steps carried out at 0.5 mL/min flow rates.

Fractions containing ERK5/MEK pooled and dialysed against Buffer E (50 mM HEPES pH 7.87, 150 mM NaCl, 25% glycerol, 5 mM DTT), filter sterilised and 250 µL aliquots frozen at -80 °C.

Batch variable yield from 75 – 240 µg/ml (440 µg – 1069 µg total protein) of ERK5/MEK complex.

Biochemical ERK5 activity assay. Compound IC_{50}s were determined against ERK5 using FAM-EGFR-derived peptide substrate (LVEPLTPSGEAPNQ(K-5FAM)-COOH, Molecular Devices #R7129) and an IMAP FP Progressive Binding System kit (Molecular Devices #R8127). Compounds were serially diluted 3-fold to generate 10-point curves. Assays were incubated for 2 h at 37 °C in a 10 µL reaction volume containing ERK5 (5-10 nM depending on batch activity), 1x IMAP reaction buffer, 1mM DTT, 250 nM peptide substrate, 300 µM ATP and 4% DMSO. Detection of phosphorylated product was performed by transferring 1 µL of the enzyme reaction above with 9 µL of 1x IMAP reaction buffer and 30 µL of IMAP Binding Solution, prepared as per the manufacturer's instructions, and incubating for 2 h at RT. Fluorescence polarisation was measured on a Pherastar (BMG) using an FP 485-520-520 optic module.

Biochemical p38 activity assay. Compound IC_{50}s were determined against full length p38 protein (Millipore #14-251) in a LANCE assay format using a Ulight-MBP peptide substrate (PerkinElmer #TRF0109). Compounds were serially diluted as for the ERK5 biochemical assay. Assays were incubated for 1 h at 37 °C in a 10 µL reaction volume containing p38 (1-3 nM depending on batch activity), 50 mM Tris pH 7.5, 5mM $MgCl_2$, 0.5 mM EGTA, 2 mM DTT, 0.01% Triton X100, 50 nM peptide substrate, 350 µM ATP and 4% DMSO. Quenching of the reaction and detection of phosphorylated product were performed by addition of 10 µL of a mixture of EDTA (5 mM final concentration) and LANCE Ultra Europium-anti-phospho-MBP antibody (PerkinElmer #TRF0201, 2 nM final concentration), and incubating for 2 h at RT, protected from light. FRET was measured on a Pherastar (BMG) using an HTRF 337-665-620 optic module.

ERK5-Dependent Dual-Luciferase Reporter Assay. Given the paucity of validated ERK5 substrates we assessed cell-based activity against ERK5 using a transcriptional reporter assay in which mutationally activated MEK5 (MEK5D) was co-expressed in cells together with ERK5 and the transactivation domain of the transcription factor MEF2D (an ERK5 substrate) fused to the DNA binding domain of the yeast GAL4 protein. ERK5-dependent activity of GAL4-MEF2D was assayed using a co-expressed luciferase reporter as previously described.[30]

Plasmids. The HA-ERK5 and EGFP-MEK5D constructs have been described previously[30] and were derived from constructs provided by J.D. Lee. GAL4-MEF2D was a kind gift from J.M. McDermott and GAL4 LUC and CMV-Renilla reporters from D. Gillispie, Universidad de La Laguna, Spain.

Cell culture. HEK293 were cultured in DMEM supplemented with 10% FBS at 37 °C in an atmosphere of 5% CO_2 and 95% humidity as described previously.[30]

Luciferase assays. HEK293 were transfected using Lipofectamine 2000 (LifeTechnologies, https://www.lifetechnologies.com/uk/en/home/brands/product-brand/lipofectamine/lipofectamine-2000.html), according to the manufacturer's instructions. ERK5 inhibitors was added to a final concentrations of 30 µM, 10 µM, 3 µM, 1 µM and 0.3 µM 4 h post transfection. After a further 20 h cells were harvested and processed for firefly and renilla luciferase activity using the Dual Luciferase Reporter (Promega, http://www.promega.co.uk/products/reporter-assays-and-transfection/reporter-assays/dual_luciferase-reporter-assay-system/) assay according to the manufacturer's instructions.

Quantification of Cellular Inhibition of ERK5. Raw data was processed using Microsoft Excel and GraphPad Prism 6.02, enabling generation of IC_{50} values. Each data point is the mean of 3 values ± standard deviation.

In vivo Experiments

All *in vivo* experiments were reviewed and approved by the Newcastle University Animal Welfare and ethical review body, and performed according to the Guidelines for the Welfare set out by an *ad hoc* committee of the National Cancer Research Institute (Workman et al, 2010) and national law.

Matrigel Plug Assay Protocol. Matrigel containing basic fibroblast growth factor (bFGF), which induces angiogenesis, was injected sub-cutanously into 15 8-10 week old female CD1 mice (Charles River, Kent UK). 24 hours post Matrigel inoculation, mice were randomised to receive either vehicle, 50 mg/kg XMD8-92 i.p. twice daily for 7 days or **46** p.o. twice daily for 7 days. On day 7, mice were killed; Matrigel plugs were removed and snap frozen in liquid nitrogen. Haemoglobin was measured using the Drabkin's method. Drabkin's reagent (containing sodium bicarbonate, potassium ferricyanide and potassium cyanide) allowed quantitative colorimetric determination of haemoglobin concentrations in blood.

Human Tumour Xenograft Model Protocol. Female CD1 nude (nu/nu) mice at 8-10 week old (Charles River Kent UK) were inoculated with A2780 cells (human ovarian carcinoma) cells subcutaneously on the right flank, and tumour volume was allowed to develop for 7 days to an average volume of 72 mm^3. Mice were randomized (9 per group) to receive either vehicle, 50 mg/kg XMD8-92 i.p. or 100 mg/kg **46** p.o. twice daily for 10 days. Tumour volumes were then measured using digital calipers three times per week. Statistical analysis of mean tumour volume,

at the end of treatment, was performed using an unpaired two tailed *t*-test. Body weight was monitored as an assessment of drug toxicity.

Pharmacokinetic (PK) Studies. Female CD1 mice 8-10 week old (Charles River, Kent UK) were treated with 10 mg/kg of **46** either i.v. or p.o., and were bled by cardiac puncture under terminal anaesthesia at selected time points post-treatment (0.083-24 hours, 3 mice/time point). Blood was collected into heparinised tubes, and plasma was separated and stored at –20 °C until analysed. Drug concentrations were determined by LCMS calibrated with standards prepared in control plasma and pharmacokinetic parameters determined using a non-compartmental (trapezoidal) method. Terminal half-life was determined using log linear regression of the final six time points ($r^2 > 0.96$).

Crystallographic Protocols. Preparation of ERK5-**46** complex crystals. Purified unphosphorylated ERK5 kinase domain (residues 46-402) was purchased from Proteros Biostructures GmbH and co-crystals with compound were prepared in a similar manner as described.[31] ERK5 (46-402) at 11.5 mg mL^{-1} in storage buffer (50 mM HEPES (pH 6.5), 150 mM NaCl, 10 % (v/v) glycerol, 2 mM DTT) was mixed with **46** (100 mM in 100 % DMSO) to give a final concentration of 1 mM **46** and 1 % (v/v) DMSO. Complex formation was allowed to proceed for two hours on ice. The sample was then clarified by centrifugation (5 min, 16 000*g*, 4 ºC) immediately before use in crystallisation. Crystals were grown by sitting drop vapour diffusion at 20 ºC in 96-well MRC plates, by mixing the protein: compound complex with crystallisation buffer comprising 5 % (v/v) PEG 6000, 0.1 M MES (pH 6.0), 5 mM DTT in a 1:1 ratio to give a 0.8 µL drop. Drops were immediately streak seeded with a seed stock prepared from crystals of ERK5 with an indazole ERK5 inhibitor (in house series - unpublished structure). The seed stock was prepared by looping two crystals of the ERK5: indazole complex into 2 µL crystallisation

buffer (5 % (v/v) PEG 6000, 0.1 M MES (pH 6.0), 5 mM DTT). The buffer and crystals were transferred into a micro-centrifuge tube containing a stabilisation buffer (20 µL 5 % (v/v) PEG 6000, 0.1 M MES (pH 6.0), 5 mM DTT plus 80 µL 6 % (v/v) PEG 6000, 0.1 M MES (pH 6.25), 5 mM DTT) and the crystals were crushed by vortexing with a Teflon bead. The seed stock was aliquoted into cryo-tubes, flash frozen in liquid nitrogen, and stored at -80 ºC until use.

X-ray diffraction data collection, structure solution and refinement for the complex of ERK5 with 46. Crystals were passed briefly through a cryoprotectant solution comprising 4.9 % (v/v) PEG 6000, 70 mM MES (pH 6.0), 3.5 mM DTT, 30 % (v/v) glycerol, 1 % (v/v) DMSO and 10 mM **46** before flash cooling in liquid nitrogen. Data were collected at 100 K on beamline I04 at the DIAMOND Light Source (Oxford, UK). Data were processed using XDS,[32] and programs from the CCP4 suite[33] as implemented within autoPROC[34]. The structure was solved by molecular replacement using Molrep[35] and a high resolution structure of ERK5 (PDB ID 5BYZ[31]) as the search model. Rounds of manual model completion in Coot[36] were interspersed with maximum-likelihood TLS refinement in Buster (v. 2.10.2)[37]. Ligand libraries and coordinates were generated from the corresponding SMILES string using grade (v1.2.9, Global Phasing Ltd., Cambridge, UK) and cross-validated against the CSD[38] using Mogul[39] after fitting the ligand into difference density and reciprocal space refinement. Crystallographic data statistics are provided in Table S1.

BRD4 Expression, Purification and Surface Plasmon Resonance Protocols

Expression and purification of recombinant BRD4 bromodomain 1. Harvested bacterial cells were resuspended in lysis buffer comprising 50 mM HEPES (pH 7.4), 200 mM NaCl, 10 mM imidazole, 0.5 mg mL^{-1} lysosyme, and 0.2 mg mL^{-1} DNAse at 4 ºC for 1 h. After sonication and centrifugation (1 h at 35,000 x *g*), the supernatant was purified by immobilized Ni^{2+} ion affinity chromatography. The peak fractions were pooled and incubated with GST tagged HRV 3C protease (50:1) at 4 ºC overnight. The cleaved His-tag was separated from BRD4 by size exclusion chromatography using a Superdex 75 (26/60) column (GE Healthcare), equilibrated and run in 50 mM HEPES (pH 7.4), 200 mM NaCl and 1 mM DTT. All purification steps were performed using an ÄKTA Pure (GE Healthcare) at 4 ºC.

Surface Plasmon Resonance. SPR-based ligand binding assays were performed using a BIAcore S200 (GE Healthcare) at 25 ºC using single cycle affinity. Immobilisation of BRD4 was achieved using standard amine coupling on a CM5 chip surface. The surface was prepared through activation with EDC/NHS, followed by injection of 10 µg mL^{-1} BRD4 until a target level of 8000 RU was reached. The surface was then quenched using 1 M ethanolamine and washed with running buffer (10 mM HEPES, 150 mM NaCl, 0.01 % (v/v) TWEEN20, 0.5 mM TCEP and 1 % (v/v) DMSO) at a flow rate of 30 µL min^{-1}. XMD8-92 and **46** were injected in a dose-response manner (nine points ranging from 0-20 µM) with contact time 30sec and dissociation time 160sec in series across the reference and BRD4-immobilised flow cells using solvent correction to account for bulk refractive index changes. The reference channel response was subtracted from the BRD4-immobilised channel response and dose-response data were fitted using an affinity steady-state 1:1 binding model to determine the K_d.

Accession codes

The coordinates for the ERK5-**46** complex has been deposited in the wwPDB under accession number 5O7I.

Summary of Generic Analytical and Chromatographic Conditions. All commercial reagents were purchased from Sigma-Aldrich Chemical Company, Alfa Aesar, Apollo Scientific or Tokyo Chemical Industry UK Ltd. The chemicals were of the highest available purity. Unless otherwise stated, chemicals were used as supplied without further purification. Anhydrous solvents were obtained from AcroSealTM or Aldrich SureSeal™ bottles and were stored under nitrogen. Petrol refers to the fraction with a boiling point between 40 and 60 °C. Thin layer chromatography utilised to monitor reaction progress was conducted on plates pre-coated with silica gel Merck 60F254 or Merck NH_2F254S. The eluent was as stated (where this consisted of more than one solvent, the ratio is stated as volume:volume) and visualisation was either by short wave (254 nm) ultraviolet light, or by treatment with the visualisation reagent stated followed by heating. 'Flash' medium pressure liquid chromatography (MPLC) was carried out either on a Biotage SP4 automated purification system or a Varian 971-FP automated purification system, using pre-packed Varian or Grace silica or amino-bonded silica cartridges. All reactions carried out in a microwave were performed in a Biotage Initiator with Sixty robot. Melting points were determined using a VWR Stuart SMP40 apparatus and are uncorrected. ^{1}H, ^{13}C and ^{19}F nuclear magnetic resonance (NMR) spectra were obtained as either $CDCl_3$, MeOD or DMSO-d_6 solutions and recorded at 500 MHz, 126 MHz and 471 MHz, respectively, on a Bruker Avance III 500 spectrometer. Where ^{13}C NMR data are not quoted, insufficient material was available or problems obtaining high resolution spectra were encountered. Chemical shifts are quoted in parts per million (δ) referenced to the

appropriate deuterated solvent employed. Multiplicities are indicated by s (singlet), d (doublet), t (triplet), q (quartet), quin (quintet), m (multiplet), br (broad) or combinations thereof. Coupling constant values are given in Hz. Homonuclear and heteronuclear two dimensional NMR experiments were used where appropriate to facilitate assignment of chemical shifts. LC-MS was carried out on a Waters Acquity UPLC system with PDA and ELSD employing positive or negative electrospray modes as appropriate to the individual compound. High resolution mass spectrometry (HRMS) was performed by the EPSRC UK National Mass Spectrometry Facility, Swansea University, Singleton Park, Swansea, SA2 8PP. FTIR spectra were recorded on either a Bio-Rad FTS 3000MX diamond ATR or an Agilent Cary 630 FTIR as a neat sample. UV spectra were obtained using a U-2001 Hitachi Spectrophotometer with the sample dissolved in ethanol. The purity of compounds was assessed by high performance liquid chromatography (HPLC). All tested compounds were ≥95% purity. The HPLC instrument was an Agilent 1200 equipped with a photodiode array detector (190-400 nm). Sample temperature, ambient; injection volume, 5 μL; flow rate, 1mL/min. 5% to 100% MeCN gradient over 9 min and an isocratic hold at 100% MeCN for 2.5 min, before returning to initial conditions. Mobile phase A = 0.1% ammonia in water or 0.1% formic acid in water, mobile phase B = MeCN. Column: Waters XSELECT CSH C18, 5 μm, 4.6 mm × 150 mm. Column maintained at ambient temperature.

General Synthetic Procedures

General procedure A: To a suspension of $AlCl_3$ (2.5 eq.) in DCM (1 mL/mmol $AlCl_3$) at 0 °C was added the relevant acid chloride (2 eq.) followed by methyl 1*H*-pyrrole-2-carboxylate (1 eq.). The resulting mixture was allowed to reach RT and stirred for 16 h. The reaction was quenched at 0 °C with a 1 M aqueous solution of HCl (20 mL). The product was extracted with DCM (3 × 100

mL), washed with an aqueous saturated solution of $NaHCO_3$ (2 × 100 mL) and brine (100 mL). Combined organic layers were dried over Na_2SO_4 and concentrated *in vacuo*.

General procedure B: To a solution of pyrrole ester (1.0 eq.) in THF (8 mL/mmol) was added LiOH (20 eq.) in water (13 mL/mmol). The resulting mixture was heated at 60 °C for 18 h, cooled to RT and acidified to pH 4-5 with aq. HCl (1.0 M). The product was extracted into EtOAc (100 mL/mmol), washed with water (100 mL/mmol), brine (100 mL/mmol) and dried over Na_2SO_4. The solvent was removed under vacuum to obtain the product.

General procedure C: A solution of carbonyldiimidazole (2.0 eq.) and the required carboxylic acid (1.0 eq.) in THF (5 mL/mmol) was heated to 70 ºC for 3 h. The appropriate amine (2.5 eq.) was added and the mixture heated at 50 °C for 3 h then at RT for 16 h. The product was extracted into EtOAc (50 mL/mmol), washed with water (50 mL/mmol), brine (50 mL/mmol) and dried over Na_2SO_4. The solvent was removed under vacuum to give the crude product.

General procedure D: The appropriate carboxylic acid (1.0 equiv.) was dissolved in MeCN (5 mL/mmol pyrrole) before the relevant amine (2.5 equiv.) was added followed by phosphorus trichloride (1.0 equiv.). The mixture was heated using microwave irradiation at 150 °C for 5 min. The reaction was quenched with a few drops of H_2O and the solvent removed *in vacuo.* The residue was re-dissolved in EtOAc (50 mL/mmol pyrrole) and washed with a saturated aqueous solution of $NaHCO_3$ (50 mL/mmol pyrrole) before being extracted with EtOAc (3 × 30 mL/mmol pyrrole). The combined organic extracts were dried over Na_2SO_4, and the filtrate concentrated *in vacuo* to afford the crude product.

Compound Syntheses

Methyl-4-benzoyl-1*H*-pyrrole-2-carboxylate (7) Prepared according to general procedure A using methyl-2-pyrrole carboxylate (112 mg, 0.90 mmol), benzoyl chloride (205 μL, 1.79 mmol) and aluminium chloride (298 mg, 2.23 mmol) in DCM (2.2 mL). Purification *via* MPLC (silica; 0-40% EtOAc in petroleum ether) gave **7** as a yellow solid (199 mg, 96%); R_f 0.40 (50% EtOAc in petroleum ether); mp 148-149 °C; λ_{max} (EtOH)/nm 285, 238; IR υ_{max}/cm^{-1} 3293, 1715, 1620, 1596, 1555; ^{1}H NMR (300 MHz, DMSO-d_6) δ 3.81 (3H, s, OCH_3), 7.15 (1H, s, H-pyrrole), 7.48-7.67 (4H, m, 3 × H-Ar and H-pyrrole), 7.73-7.83 (2H, m, 2 x H-Ar), 12.76 (1H, s, NH); ^{13}C NMR (75 MHz, DMSO-d_6) δ 30.1 (OCH_3), 115.5 (CH-pyrrole), 123.2 (C), 124.2 (C), 128.0 (4 x C-Ar), 128.7 (CH-pyrrole), 131.3 (C-Ar), 138.6 (C-Ar), 160.1 (*C*OOMe), 188.6 (CO); HRMS (ES$^+$) calcd for $C_{13}H_{12}O_3N$ $[M+H]^+$ 230.0812, found 230.0811; Anal. calcd for $C_{13}H_{11}NO_3$: C, 68.11%, H, 4.84%, N, 6.11%, found: C, 68.33%, H, 4.78%, N, 6.21%.

Methyl 4-(2-fluorobenzoyl)-1*H*-pyrrole-2-carboxylate (8) Prepared according to general procedure A using methyl-2-pyrrole carboxylate (3.0 g, 24.0 mmol), 2-fluorobenzoyl chloride (5.7 mL, 48.0 mmol) and aluminium chloride (5.52 g, 60.0 mmol) in DCM (60 mL). Purification *via* precipitation (EtOAc in petroleum ether) gave **8** as a yellow solid (4.16 g, 70%); mp 129-130 °C; λ_{max} (EtOH)/nm 284, 234; IR υ_{max}/cm^{-1} 3291, 1722, 1632, 1553; ^{1}H NMR (300 MHz, DMSO-d_6) δ 3.79 (3H, s, OCH_3), 7.06 (1H, s, H-pyrrole), 7.27-7.37 (2H, m, H-pyrrole and H-Ar), 7.40-7.66 (3H, m, 3 x H-Ar), 12.79 (1H, s, NH); ^{13}C NMR (75 MHz, DMSO-d_6) δ 51.1 (OCH_3), 114.8 (CH-pyrrole), 115.8 (d, $J_{C\text{-}F}$ = 21.5 Hz, C-Ar), 123.6 (C), 124.1 (d, $J_{C\text{-}F}$ = 3.3 Hz, C-Ar), 125.2 (C), 127.7 (d, $J_{C\text{-}F}$ = 15.3 Hz, C), 129.1 (CH-pyrrole), 129.2 (d, $J_{C\text{-}F}$ = 3.1 Hz, C-Ar), 132.2 (d, $J_{C\text{-}F}$ = 8 Hz, ArH), 158.5 (d, $J_{C\text{-}F}$ = 247.3 Hz, C-F), 160.0 (*C*OOMe), 185.6 (CO); HRMS (ES$^+$) calcd for

$C_{13}H_{10}FNO_3$ $[M+H]^+$ 248.0717, found 248.0717; Anal. calcd for $C_{13}H_{10}FNO_3$: C, 63.16%, H, 4.08%, N, 5.67%, found: C, 63.31%, H, 3.92%, N, 5.51%.

Methyl 4-(3-fluorobenzoyl)-1*H*-pyrrole-2-carboxylate (9) Prepared according to general procedure A using methyl-2-pyrrole carboxylate (400 mg, 3.20 mmol), 3-fluorobenzoyl chloride (0.76 mL, 6.40 mmol) and aluminium chloride (766 mg, 7.99 mmol) in DCM (8 mL). Purification *via* MPLC (silica; 0-10% EtOAc in petroleum ether) gave **9** as a pale yellow solid (585 mg, 74%); R_f 0.16 (20% EtOAc in petroleum ether); mp 128-130 ºC; λ_{max} (EtOH)/nm 286, 238; IR υ_{max}/cm^{-1} 3302, 1716, 1624; ^{1}H NMR (300 MHz, DMSO-d_6) δ 3.82 (3H, s, CH_3), 7.17 (1H, s, H-pyrrole), 7.46-7.50 (1H, m, H-Ar), 7.53-7.56 (1H, m, H-Ar), 7.58-7.65 (2H, m, 2 × H-Ar), 7.63 (1H, s, H-pyrrole), 12.79 (1H, s br, NH); ^{13}C NMR (75 MHz, DMSO-d_6) δ 51.8, 115.1, 115.4, 116.2, 118.8, 119.1, 124.2, 124.6, 124.9, 129.8, 131.0, 131.1, 141.5, 160.8, 162.5, 187.9; ^{19}F NMR (470 MHz, DMSO-d_6) δ -112.3; MS (ES+) *m/z* 248.8 $[M+H]^+$.

Methyl 4-(4-fluorobenzoyl)-1*H*-pyrrole-2-carboxylate (10) Prepared according to general procedure A using methyl-2-pyrrole carboxylate (400 mg, 3.20 mmol), 4-fluorobenzoyl chloride (0.76 mL, 6.4 mmol) and aluminium chloride (766 mg, 7.99 mmol) in DCM (8 mL). Purification *via* MPLC (silica; 0-10% EtOAc in petroleum ether) gave **10** as a yellow solid (595 mg, 75%); R_f 0.12 (20% EtOAc in petroleum ether); mp 154-156 ºC; λ_{max} (EtOH)/nm 285, 237; IR υ_{max}/cm^{-1} 1724, 1627; ^{1}H NMR (300 MHz, DMSO-d_6) δ 3.82 (3H, s, CH_3), 7.16 (1H, s, H-pyrrole), 7.35-7.38 (2H, m, 2 × H-Ar), 7.60 (1H, s, H-pyrrole), 7.87-7.90 (2H, m, 2 × H-Ar), 12.76 (1H, s br, NH); ^{13}C NMR (75 MHz, DMSO-d_6) δ 51.5, 115.5, 115.9, 123.6, 124.2, 129.4, 131.4, 135.3, 160.5, 164.2, 187.5; ^{19}F NMR (470 MHz, DMSO-d_6) δ -107.9; MS (ES+) *m/z* 248.9 $[M+H]^+$.

Methyl 4-(2-chlorobenzoyl)-1*H*-pyrrole-2-carboxylate (11) Prepared according to general procedure A using methyl-2-pyrrole carboxylate (400 mg, 3.20 mmol), 2-chlorobenzoyl chloride

(0.81 mL, 6.40 mmol) and aluminium chloride (766 mg, 7.99 mmol) in DCM (8 mL). Purification *via* MPLC (silica; 0-10% EtOAc in petroleum ether) gave **11** as a beige solid (630 mg, 74%); R_f 0.12 (20% EtOAc in petroleum ether); mp 137-139 ºC; λ_{max} (EtOH)/nm 346, 283, 232; IR υ_{max}/cm^{-1} 3192, 1710, 1619; ^{1}H NMR (300 MHz, DMSO-d_6) δ 3.79 (3H, s, CH_3), 6.98 (1H, dd, J = 1.8 and 2.5 Hz, H-pyrrole), 7.40 (1H, dd, J = 1.8 and 3.3 Hz, H-pyrrole), 7.44-4.49 (2H, m, 2 × H-Ar), 7.52-7.55 (1H, m, H-Ar), 7.56-7.58 (1H, m, H-Ar), 12.80 (1H, s br, NH); ^{13}C NMR (125 MHz, DMSO-d_6) δ 51.6, 115.2, 124.1, 125.2, 127.1, 128.5, 129.4, 129.9, 130.0, 131.2, 139.2, 160.4, 188.1; MS (ES+) *m/z* 264.3 $[M+H]^+$.

Methyl 4-(3-chlorobenzoyl)-1*H*-pyrrole-2-carboxylate (12) Prepared according to general procedure A using methyl-2-pyrrole carboxylate (400 mg, 3.20 mmol), 3-chlorobenzoyl chloride (0.82 mL, 6.4 mmol) and aluminium chloride (766 mg, 7.99 mmol) in DCM (8 mL). Purification *via* MPLC (silica; 0-10% EtOAc in petroleum ether) gave **12** as an off-white solid (490 mg, 60%); R_f 0.45 (50% EtOAc in petroleum ether); mp 126-128 ºC; λ_{max} (EtOH)/nm 288, 237; IR υ_{max}/cm^{-1} 1724, 1624; ^{1}H NMR (500 MHz, DMSO-d_6) δ 3.82 (3H, s, OCH_3), 7.16 (1H, s, H-pyrrole), 7.58 (1H, dd, J = 7.9 and 8.0 Hz, H-Ar), 7.63 (1H, s, H-pyrrole), 7.70-7.71 (1H, m, H-Ar), 7.74-7.76 (2H, m, 2 × H-Ar), 12.81 (1H, s br, NH); ^{13}C NMR (125 MHz, DMSO-d_6) δ 51.6, 115.8, 123.8, 124.9, 127.2, 128.0, 129.8, 130.6, 131.7, 133.4, 140.7, 160.5, 187.6; MS (ES+) *m/z* 262.0 $[M+H]^+$.

Methyl 4-(4-chlorobenzoyl)-1*H*-pyrrole-2-carboxylate (13) Prepared according to general procedure A using methyl-2-pyrrole carboxylate (400 mg, 3.20 mmol), 4-chlorobenzoyl chloride (0.82 mL, 6.40 mmol) and aluminium chloride (766 mg, 7.99 mmol) in DCM (8 mL). Purification *via* MPLC (silica; 0-10% EtOAc in petroleum ether) gave **13** as a beige solid (690 mg, 82%); R_f 0.12 (20% EtOAc in petroleum ether); mp 176-178 ºC; λ_{max} (EtOH)/nm 244; IR υ_{max}/cm^{-1} 3169, 1716, 1620; ^{1}H NMR (300 MHz, DMSO-d_6) δ 3.81 (3H, s, CH_3), 7.16 (1H, s, H-pyrrole), 7.60

(2H, d, J = 8.4 Hz, 2 × H-Ar), 7.61 (1H, s, H-pyrrole), 7.81 (2H, d, J = 8.4 Hz, 2 × H-Ar), 12.78 (1H, s br, NH); ^{13}C NMR (75 MHz, DMSO-d_6) δ 51.8, 116.2, 124.1, 124.6, 129.0, 129.7, 130.7, 137.1, 137.9, 160.8, 188.1; MS (ES+) *m/z* 264.4 $[M+H]^+$.

Methyl 4-(2,3-difluorobenzoyl)-1*H*-pyrrole-2-carboxylate (14) Prepared according to general procedure A using methyl-2-pyrrole carboxylate (400 mg, 3.20 mmol), 2,3-difluorobenzoyl chloride (1.13 g, 0.80 mL, 6.4 mmol) and aluminium chloride (766 mg, 7.99 mmol) in DCM (8 mL). Purification *via* MPLC (silica; 0-10% EtOAc in petroleum ether) gave **14** as a yellow solid (250 mg, 30%); R_f 0.13 (20% EtOAc in petroleum ether); mp 159-160 ºC; λ_{max} (EtOH)/nm 379, 286, 234; IR υ_{max}/cm^{-1} 3323, 1720, 1631; ^{1}H NMR (300 MHz, DMSO-d_6) δ 3.87 (3H, s, CH_3), 7.11 (1H, s, H-pyrrole), 7.33-7.38 (2H, m, 2 × H-Ar), 7.60 (1H, s, H-pyrrole), 7.61-7.68 (1H, m, H-Ar), 12.85 (1H, s br, NH); ^{13}C NMR (75 MHz, DMSO-d_6) δ 51.6, 115.5, 119.6, 124.1, 124.8, 125.1, 125.2, 129.8, 130.4, 146.8, 149.7, 160.4, 184.7; ^{19}F NMR (470 MHz, DMSO-d_6) δ -137.7, -141.3; MS (ES+) *m/z* 264.0 $[M-H]^-$.

Methyl 4-(2,6-difluorobenzoyl)-1*H*-pyrrole-2-carboxylate (15) Prepared according to general procedure A using methyl-2-pyrrole carboxylate (400 mg, 3.20 mmol), 2,6-difluorobenzoyl chloride (1.13 g, 0.80 mL, 6.4 mmol) and aluminium chloride (766 mg, 7.99 mmol) in DCM (8 mL). Purification *via* MPLC (silica; 0-10% EtOAc in petroleum ether) gave **15** as an orange solid (180 mg, 22%); R_f 0.17 (20% EtOAc in petroleum ether); mp 132-124 ºC; λ_{max} (EtOH)/nm 279, 264; IR υ_{max}/cm^{-1} 1732, 1624; ^{1}H NMR (500 MHz, DMSO-d_6) δ 3.57 (3H, s, CH_3), 7.04 (1H, s, H-pyrrole), 7.23-7.28 (2H, m, 2 × H-Ar), 7.58 (1H, s, H-pyrrole), 7.59-7.67 (1H, m, H-Ar), 12.79 (1H, s br, NH); ^{13}C NMR (125 MHz, DMSO-d_6) δ 51.6, 112.2, 114.6, 117.5, 124.5, 125.9, 130.14, 132.3, 158.7, 160.3, 181.6; ^{19}F NMR (470 MHz, DMSO-d_6) δ -114.1; MS (ES+) *m/z* 266.5 $[M+H]^+$.

Methyl 4-(2,6-dichlorobenzoyl)-1*H*-pyrrole-2-carboxylate (16) Prepared according to general procedure A using methyl-2-pyrrole carboxylate (400 mg, 3.20 mmol), 2,6-dichlorobenzoyl chloride (0.92 mL, 6.40 mmol) and aluminium chloride (766 mg, 7.99 mmol) in DCM (8 mL). Purification *via* MPLC (silica; 0-10% EtOAc in petroleum ether) gave **16** as a white solid (700 mg, 73%); R_f 0.19 (20% EtOAc in petroleum ether); mp 184-186 ºC; λ_{max} (EtOH)/nm 282, 226; IR υ_{max}/cm^{-1} 3219, 1726, 1641; ^{1}H NMR (300 MHz, DMSO-d_6) δ 3.79 (3H, s, CH_3), 6.96 (1H, d, J = 1.6 Hz, H-pyrrole), 7.49 (1H, d, J = 1.6 Hz, H-pyrrole), 7.52-7.55 (1H, m, H-Ar), 7.58-7.60 (2H, m, 2 ×H-Ar), 12.87 (1H, s br, NH); ^{13}C NMR (125 MHz, DMSO-d_6) δ 51.6, 114.6, 124.5, 124.6, 128.5, 129.9, 130.4, 131.5, 138.0, 160.2, 185.6; MS (ES+) *m/z* 298.1 $[M+H]^+$.

Methyl 4-(2-chloro-6-fluorobenzoyl)-1*H*-pyrrole-2-carboxylate (17) Prepared according to general procedure A using methyl-2-pyrrole carboxylate (3.00 g, 23.80 mmol), 2-chloro-6-fluorobenzoyl chloride (6.40 mL, 47.60 mmol) and aluminium trichloride (7.93 g, 59.50 mmol) in DCM (40 mL). Purification *via* MPLC (silica; 0-80% EtOAc in petroleum ether) gave **17** as a white solid (4.20 g, 63%); R_f 0.48 (50% EtOAc in petroleum ether); mp 183-184 °C; λ_{max} (EtOH)/nm 282, 232; IR υ_{max}/cm^{-1} 3224, 1732, 1639, 1563; ^{1}H NMR (500 MHz, DMSO-d_6) δ 7.00 (1H, s, H-3), 7.37-7.40 (1H, m, H-5'), 7.46 (1H, d, J = 8.3 Hz, H-3'), 7.54 (1H, dd, J = 1.5 and 3.3 Hz, H-5), 7.58 (1H, ddd, J = 6.3, 8.3 and 8.3 Hz, H-4'); ^{13}C NMR (125 MHz, DMSO-d_6) δ 51.7, 114.6, 115.0, 124.5, 125.3, 125.8, 127.8, 130.1, 130.3, 131.9, 158.6, 160.2, 183.7; ^{19}F NMR (470 MHz, DMSO-d_6) δ -114.0; HRMS *m/z* calcd for $C_{13}H_{10}{}^{35}ClFNO_3$ $[M+H]^+$ 282.0328, found 282.0331.

Methyl 4-(2-bromo-6-fluorobenzoyl)-1*H*-pyrrole-2-carboxylate (18) Prepared according to general procedure A using methyl-2-pyrrole carboxylate (429 mg, 3.43 mmol), 2-bromo-6-fluorobenzoylchloride (1.62 g, 6.85 mmol), aluminium trichloride (1.15 g, 8.56 mmol) in DCM

(10 mL). Purification *via* MPLC (silica; 0-50% EtOAc in petroleum ether) gave **18** as a white solid (760 mg, 68%); R_f 0.51 (50% EtOAc in petroleum ether); mp 185-186 °C; λ_{max} (EtOH)/nm 280; IR υ_{max}/cm^{-1} 3229, 1731, 1638, 1563; ^{1}H NMR (500 MHz, DMSO-d_6) δ 3.80 (3H, s, CH_3), 7.00 (1H, s, H-3), 7.39-7.43 (1H, m, H-5'), 7.50 (1H, ddd, *J* = 6.3, 8.3 and 8.3 Hz, H-4'), 7.52 (1H, s, H-5), 7.59 (1H, d, *J* = 8.3 Hz, H-3'), 12.90 (1H, br s, NH); ^{13}C NMR (125 MHz, DMSO-d_6) δ 51.6, 114.7, 115.4, 118.9, 124.5, 125.0, 128.8, 130.4, 132.2, 158.4, 160.3, 184.6; ^{19}F NMR (470 MHz, DMSO-d_6) δ -113.6; HRMS *m/z* calcd for $C_{13}H_{10}{}^{79}BrFNO_3$ $[M+H]^+$ 325.9823, found 325.9830.

4-Benzoyl-1*H*-pyrrole-2-carboxylic acid (19) Prepared according to general procedure B using methyl 4-benzoyl-1*H*-pyrrole-2-carboxylate **7** (184 mg, 0.80 mmol), LiOH (676 mg, 16.1 mmol) in THF/H_2O (5.0 mL/4.0 mL) to give **19** as a pale pink solid (161 mg, 94%); R_f 0.67 (10% MeOH and 10% AcOH in DCM); mp 225-226 °C; λ_{max} (EtOH)/nm 285, 237; IR υ_{max}/cm^{-1} 3333, 1667, 1624, 1549; ^{1}H NMR (300 MHz, DMSO-d_6) δ 7.11 (1H, s, H-pyrrole), 7.44-7.67 (4H, m, 3 × H-Ar and H-pyrrole), 7.72-7.84 (2H, m, 2 × H-Ar), 12.55 (1H, s, NH); ^{13}C NMR (75 MHz, DMSO-d_6) δ 115.1 (CH-pyrrole), 124.1 (C), 124.6 (C), 128.1 (4 x C-Ar), 128.4 (CH-pyrrole), 131.4 (C-Ar), 138.8 (C-Ar), 161.1 (*C*OOMe), 188.8 (CO); HRMS (ES^+) calcd for $C_{12}H_9NO_3$ $[M+H]^+$ 216.0655, found 216.0655; Anal. calcd for $C_{12}H_9NO_3$: C, 66.97%, H, 4.22%, N, 6.51%, found: C, 66.81%, H, 4.17%, N, 6.33%.

4-(2-Fluorobenzoyl)-1*H*-pyrrole-2-carboxylic acid (20) Prepared according to general procedure B using methyl 4-(2-fluorobenzoyl)-1*H*-pyrrole-2-carboxylate **8** (2.0 g, 8.1 mmol), LiOH (3.9 g, 162 mmol) in THF/H_2O (30 mL/50 mL) to give **20** as a pale pink solid (1.28 g, 68%); mp 181-182 °C, λ_{max} (EtOH)/nm 284, 234. IR υ_{max}/cm^{-1} 3339, 3301, 1688, 1630, 1561, 1483; ^{1}H NMR (300 MHz, DMSO-d_6) δ 7.01 (1H, s, H-pyrrole), 7.25-7.39 (2H, m, 2 x H-Ar), 7.43 (1H, s,

H-pyrrole), 7.49-7.66 (2H, m, 2 x H-Ar), 12.61 (1H, s, NH), 12.87 (1H, s, OH); ^{13}C NMR (75 MHz, DMSO-d_6) δ 114.5 (CH-pyrrole), 115.8 (d, $J_{C\text{-}F}$ = 21.5 Hz, C-Ar), 124.2 (d, $J_{C\text{-}F}$ = 3.2 Hz, C-Ar), 124.9 (C), 125.2 (C), 127.8 (d, $J_{C\text{-}F}$ = 15.8 Hz, C), 128.8 (CH-pyrrole), 129.3 (d, $J_{C\text{-}F}$ = 3.0 Hz, C-Ar), 132.2 (d, $J_{C\text{-}F}$ = 8.3 Hz, ArH), 158.5 (d, $J_{C\text{-}F}$ = 247.0 Hz, C-F), 161.0 (COOH), 185.7 (CO); HRMS (ES$^+$) calcd for $C_{12}H_8NO_3F$ $[M+H]^+$ 234.0561, found 234.0561.

4-(3-Fluorobenzoyl)-1*H*-pyrrole-2-carboxylic acid (21) Prepared according to general procedure B using: methyl 4-(3-fluorobenzoyl)-1*H*-pyrrole-2-carboxylate **9** (200 mg, 0.81 mmol), LiOH (1.55 g, 16.2 mmol) in THF/H_2O (5.5 mL/8.2 mL) to give **21** as an orange solid (185 mg, 98%); R_f 0.06 (10% MeOH in EtOAc); mp 218-219 ºC; λ_{max} (EtOH)/nm 289, 237; IR υ_{max}/cm^{-1} 3238, 1692, 1613; ^{1}H NMR (300 MHz, DMSO-d_6) δ 7.11 (1H, m, H-pyrrole), 7.45-7.50 (1H, m, H-Ar), 7.52-7.55 (1H, m, H-Ar), 7.56 (1H, dd, J = 1.5 and 3.1 Hz, H-pyrrole), 7.57-7.64 (2H, m, 2 × H-Ar), 12.60 (1H, s br, NH), 12.85 (1H, s, COOH); ^{13}C NMR (75 MHz, DMSO-d_6) δ 115.1, 115.4, 115.7, 118.7, 119.0, 124.4, 124.9, 125.5, 129.4, 130.9, 131.1, 141.6, 141.7, 161.7, 162.3, 185.1; ^{19}F NMR (470 MHz, DMSO-d_6) δ -112.3; MS (ES+) *m/z* 235.2 $[M+H]^+$.

4-(4-Fluorobenzoyl)-1*H*-pyrrole-2-carboxylic acid (22) Prepared according to general procedure B using methyl 4-(4-fluorobenzoyl)-1*H*-pyrrole-2-carboxylate **10** (300 mg, 1.2 mmol), LiOH (2.33 g, 24.3 mmol) in THF/H_2O (7.0 mL/10.5 mL) to give **22** as an off-white solid (110 mg, 40%); R_f 0.07 (EtOAc); mp: 224-225 ºC; λ_{max} (EtOH)/nm 253, 236; IR υ_{max}/cm^{-1} 3372, 1667, 1622; ^{1}H NMR (300 MHz, DMSO-d_6) δ 7.06 (1H, s, H-pyrrole), 7.32-7.38 (2H, m, 2 × H-Ar), 7.49 (1H, s, H-pyrrole), 7.85-7.89 (2H, m, 2 × H-Ar), 12.49 (1H, s br, NH), 13.00 (1H, s br, COOH); ^{13}C NMR (75 MHz, DMSO-d_6) δ 114.8, 115.5, 124.0, 128.5, 131.3, 135.5, 161.7, 164.1, 187.7; ^{19}F NMR (470 MHz, DMSO-d_6) δ -108.2; MS (ES-) *m/z* 232.1 $[M-H]^-$.

4-(2-Chlorobenzoyl)-1*H*-pyrrole-2-carboxylic acid (23) Prepared according to general procedure B using methyl 4-(2-chlorobenzoyl)-1*H*-pyrrole-2-carboxylate **11** (230 mg, 0.76 mmol), LiOH (1.45 g, 15.2 mmol) in THF/H_2O (5.5 mL/8.2 mL) to give **23** as an off-white solid (155 mg, 82%); R_f 0.32 (10% MeOH in EtOAc); mp 219-220 ºC; λ_{max} (EtOH)/nm 283, 232, 211; IR υ_{max}/cm^{-1} 3294, 1668, 1636; ^{1}H NMR (500 MHz, DMSO-d_6) δ 6.94 (1H, d, *J* = 1.6 and 2.2 Hz, H-pyrrole), 7.31 (1H, d, *J* = 1.6 and 3.3 Hz, H-pyrrole), 7.44-7.49 (2H, m, 2 × H-Ar), 7.52-7.55 (1H, m, H-Ar), 7.57-7.58 (1H, m, H-Ar), 12.61 (1H, s br, NH), 12.88 (1H, s, COOH); ^{13}C NMR (125 MHz, DMSO-d_6) δ 114.7, 125.1, 125.4, 127.1, 128.5, 129.4, 129.5, 129.8, 131.1, 139.3, 161.4, 188.2; MS (ES+) *m/z* 250.3 $[M+H]^+$.

4-(3-Chlorobenzoyl)-1*H*-pyrrole-2-carboxylic acid (24) Prepared according to general procedure B using methyl 4-(3-chlorobenzoyl)-1*H*-pyrrole-2-carboxylate **12** (300 mg, 1.14 mmol), LiOH (2.2 g, 23 mmol) in THF/H_2O (8.3 mL/12.4 mL) to give **24** as an off-white solid (130 mg, 47%); R_f 0.09 (10% MeOH in EtOAc); mp 282-284 ºC; λ_{max} (EtOH)/nm 288, 236; IR υ_{max}/cm^{-1} 3335, 1628, 1562; ^{1}H NMR (500 MHz, DMSO-d_6) δ 6.96 (1H, d, *J* = 1.9 Hz, H-pyrrole), 7.42 (1H, d, *J* = 1.9 Hz, H-pyrrole), 7.55-7.58 (1H, m, H-Ar), 7.67-7.69 (1H, m, H-Ar), 7.72-7.74 (2H, m, 2 × H-Ar); ^{13}C NMR (125 MHz, DMSO-d_6) δ 113.2, 123.4, 127.1, 127.8, 127.9, 130.4, 131.3, 133.2, 141.2, 162.4, 187.8; MS (ES-) *m/z* 247.9 $[M-H]^-$.

4-(4-Chlorobenzoyl)-1*H*-pyrrole-2-carboxylic acid (25) Prepared according to general procedure B using methyl 4-(4-chlorobenzoyl)-1*H*-pyrrole-2-carboxylate **13** (240 mg, 0.76 mmol), LiOH (1.45 g, 15.2 mmol) in THF/H_2O (5.5 mL/8.2 mL) to give **25** as an off-white solid (140 mg, 74%); R_f 0.24 (10% MeOH in EtOAc); mp 245-246 ºC; λ_{max} (EtOH)/nm 242; IR υ_{max}/cm^{-1} 3207, 1672, 1626; ^{1}H NMR (300 MHz, DMSO-d_6) δ 7.10 (1H, s, H-pyrrole), 7.54 (1H, s, H-pyrrole), 7.60 (2H, d, *J* = 8.4 Hz, 2 × H-Ar), 7.81 (2H, d, *J* = 8.4 Hz, 2 × H-Ar), 12.59 (1H, s br, NH), 12.86

(1H, s br, COOH); ^{13}C NMR (125 MHz, DMSO-d_6) δ 115.4, 124.0, 125.0, 128.6, 129.1 (CH-pyrrole), 130.4 (CH-Ar), 136.6, 137.5, 161.5 (C=O), 187.8 (C=O); MS (ES+) *m/z* 250.2 $[M+H]^+$.

4-(2,3-Difluorobenzoyl)-1*H*-pyrrole-2-carboxylic acid (26) Prepared according to general procedure B using methyl 4-(2,3-difluorobenzoyl)-1*H*-pyrrole-2-carboxylate **14** (250 mg, 0.9 mmol), LiOH (1.81 g, 19 mmol) in THF/H_2O (5.0 mL/7.5 mL) to give **26** as an off-white solid (165 mg, 70%); R_f 0.24 (10% MeOH in EtOAc); mp 210-211 ºC; λ_{max} (EtOH)/nm 284, 234; IR υ_{max}/cm^{-1} 3319, 2980, 1668, 1630; ^{1}H NMR (300 MHz, DMSO-d_6) δ 7.05 (1H, s, H-pyrrole), 7.33-7.37 (2H, m, 2 × H-Ar), 7.52 (1H, s, H-pyrrole), 7.58-7.66 (1H, m, H-Ar), 12.61 (1H, s br, NH), 12.98 (1H, s br, COOH); ^{13}C NMR (75 MHz, DMSO-d_6) δ 114.6, 119.4, 124.7, 124.9, 125.2, 125.6, 129.9, 130.0, 146.7, 149.8, 161.4, 184.6; ^{19}F NMR (470 MHz, DMSO-d_6) δ -137.7, -141.4; MS (ES-) *m/z* 250.0 $[M-H]^-$.

4-(2,6-Difluorobenzoyl)-1*H*-pyrrole-2-carboxylic acid (27) Prepared according to general procedure B using methyl 4-(2,6-difluorobenzoyl)-1*H*-pyrrole-2-carboxylate **15** (160 mg, 0.7 mmol), LiOH (1.29 g, 13.5 mmol) in THF/H_2O (4.5 mL/6.8 mL) to give **27** as a pale orange solid (110 mg, 65%); R_f 0.25 (10% MeOH in EtOAc); mp 197-199 ºC; λ_{max} (EtOH)/nm 392, 281, 232; IR υ_{max}/cm^{-1} 3352, 2921, 1689, 1623; ^{1}H NMR (500 MHz, DMSO-d_6) δ 6.99 (1H, s, H-pyrrole), 7.23-7.27 (2H, m, 2 × H-Ar), 7.50 (1H, s, H-pyrrole), 7.61-7.64 (1H, m, H-Ar), 12.70 (1H, s br, NH), 12.96 (1H, s br, COOH); ^{13}C NMR (125 MHz, DMSO-d_6) δ 112.2, 114.0, 117.6, 125.8, 126.1, 129.6, 132.2, 158.6, 161.4, 181.6; ^{19}F NMR (470 MHz, DMSO-d_6) δ -114.2; HRMS calcd. for $C_{12}H_8NF_2O_3$ $[M+H]^+$ 252.0467, found 252.0470.

4-(2,6-Dichlorobenzoyl)-1*H*-pyrrole-2-carboxylic acid (28) Prepared according to general procedure B using methyl 4-(2,6-dichlorobenzoyl)-1*H*-pyrrole-2-carboxylate **16** (300 mg, 1.00 mmol), LiOH (1.92 g, 20.0 mmol) in THF/H_2O (7.0 mL/10.5 mL) to give **28** as an off-white solid

(265 mg, 93%); R_f 0.06 (10% MeOH in EtOAc); mp 268-270 ºC; λ_{max} (EtOH)/nm 279, 233; IR υ_{max}/cm^{-1} 3286, 1703, 1641; ^{1}H NMR (300 MHz, DMSO-d_6) δ 6.92 (1H, s, H-pyrrole), 7.41 (1H, s, H-pyrrole), 7.49-7.53 (1H, m, H-Ar), 7.58-7.59 (2H, m, 2 × H-Ar), 12.68 (1H, s br, NH), 12.91 (1H, s, COOH); ^{13}C NMR (75 MHz, DMSO-d_6) δ 114.2, 124.5, 125.8, 128.4, 129.5, 130.5, 131.4, 138.1, 161.3, 185.6; MS (ES+) *m/z* 284.0 $[M+H]^+$.

4-(2-Chloro-6-fluorobenzoyl)-1*H*-pyrrole-2-carboxylic acid (29) Prepared according to general procedure B using methyl 4-(2-chloro-6-fluorobenzoyl)-1*H*-pyrrole-2-carboxylate **17** (4.00 g, 14.20 mmol), LiOH (6.81 g, 284.00 mmol) in THF/H_2O (100 mL/150 mL) to give **29** as a white solid (3.75 g, 99%); R_f 0.36 (5% MeOH in EtOAc); mp 209-210 °C; λ_{max} (EtOH)/nm 281, 233; IR υ_{max}/cm^{-1} 3306, 1638, 1556; ^{1}H NMR (500 MHz, DMSO-d_6) δ 6.95 (1H, s, H-3), 7.35-7.40 (1H, m, H-5'), 7.44-7.46 (2H, m, H-3' and H-5), 7.57 (1H, ddd, *J* = 6.4, 8.4 and 8.6 Hz, H-4'), 12.69 (1h, s br, NH); ^{13}C NMR (125 MHz, DMSO-d_6) δ 114.0, 114.9, 125.2, 125.2, 126.1, 127.8, 129.5, 130.3, 131.8, 158.5, 161.4, 183.7; ^{19}F NMR (470 MHz, DMSO-d_6) δ -114.0; HRMS *m/z* calcd for $C_{12}H_6{}^{35}ClFNO_3$ $[M-H]^-$ 266.0026, found 266.0019.

4-(2-Bromo-6-fluorobenzoyl)-1*H*-pyrrole-2-carboxylic acid (30) Prepared according to general procedure B using methyl 4-(2-bromo-6-fluorobenzoyl)-1*H*-pyrrole-2-carboxylate **18** (1.00 g, 3.06 mmol), LiOH (1.46 g, 61.12 mmol) in THF/H_2O (25 mL/40 mL) to give **30** as a white solid (949 mg, 99%); R_f 0.40 (5% MeOH in EtOAc); mp 210-211 °C; λ_{max} (EtOH)/nm 281; IR υ_{max}/cm^{-1} 3342, 1690, 1648, 1561; ^{1}H NMR (500 MHz, DMSO-d_6) δ 6.94 (1H, s, H-3), 7.39-7.43 (2H, m, H-5 and H-5'), 7.50 (1H, ddd, *J* = 6.3, 8.4 and 8.4 Hz, H-4'), 7.59 (1H, d, *J* = 8.4 Hz, H-Ar), 12.69 (1H, s br, NH), 12.81 (1H, s br, COOH); ^{13}C NMR (125 MHz, DMSO-d_6) δ 114.1, 115.3, 118.9, 124.9, 126.0, 128.8, 129.6, 129.8, 132.1, 158.3, 161.3, 184.6; ^{19}F NMR (470 MHz, DMSO-d_6) δ -113.8; HRMS *m/z* calcd for $C_{12}H_6{}^{79}BrFNO_3$ $[M-H]^-$ 309.9521, found 309.9516.

4-(Benzoyl)-*N*-(pyridin-4-ylmethyl)-1*H*-pyrrole-2-carboxamide (31) Prepared according to general procedure C using 4-(benzoyl)-1*H*-pyrrole-2-carboxylic acid **19** (100 mg, 0.47 mmol), carbonyl diimidazole (151 mg, 0.93 mmol) and 3-picolylamine (0.12 mL, 1.08 mmol) in THF (4 mL). Purification *via* MPLC (silica; 5-10% MeOH in EtOAc) gave **31** as a white solid (56 mg, 40%); mp 234-235 ºC; λ_{max} (EtOH)/nm 289, 242; IR υ_{max}/cm^{-1} 3321, 3202, 3105, 1612, 1565, 1535; ^{1}H NMR (300 MHz, DMSO-d_6) δ 4.47 (2H, d, J = 5.4 Hz, CH_2), 7.30 (2H, d, J = 4.5 Hz, 2 x H-Ar), 7.40 (s, 1H, H-pyrrole), 7.44 (1H, s, H-pyrrole), 7.48-7.67 (3H, m, 3 x H-Ar), 7.79 (2H, d, J = 7.8 Hz, 2 x H-Ar), 8.51 (2H, d, J = 4.2 Hz, 2 x H-Ar), 8.97 (1H, m, NH), 12.35 (1H, s, NH); ^{13}C NMR (75 MHz, DMSO-d_6) δ 40.9 (CH_2), 111.2 (CH-pyrrole), 121.8 (2 x CH-Ar), 123.8 (C), 127.2 (C), 128.0 (5 x CH-Ar), 131.1 (CH-pyrrole), 139.0 (C-Ar), 148.1 (C-Ar), 149.1 (2 x CH-Ar), 160.0 (CON), 188.9 (CO); HRMS (ES$^+$) calcd for $C_{18}H_{15}N_3O_2$ $[M+H]^+$ 306.1237, found 306.1242; Anal. calcd for $C_{18}H_{15}N_3O_2$: C, 70.81%, H, 4.95%, N, 13.76%, found: C, 70.89%, H, 4.61%, N, 13.67%.

4-(2-Fluorobenzoyl)-*N*-(pyridin-4-ylmethyl)-1*H*-pyrrole-2-carboxamide (32) Prepared according to general procedure C using 4-(2-fluorobenzoyl)-1*H*-pyrrole-2-carboxylic acid **20** (100 mg, 0.43 mmol), carbonyl diimidazole (140 mg, 0.86 mmol) and 4-picolylamine (0.11 mL, 1.07 mmol) in THF (4 mL). Purification *via* MPLC (silica; 2-10% MeOH in EtOAc) gave **32** as a white solid (94 mg, 68%); mp 226-227 ºC; λ_{max} (EtOH)/nm 287, 238; IR υ_{max}/cm^{-1} 3370, 3173, 1605, 1568, 1532, 1480; ^{1}H NMR (300 MHz, DMSO-d_6) δ 4.46 (2H, d, J = 5.7 Hz, CH_2), 7.23-7.42 (6H, m, 2 x H-pyrrole and 4 x H-Ar), 7.49-7.65 (2H, m, 2 x H-Ar), 8.50 (2H, d, J = 4.5 Hz, 2 x H-Ar), 8.97 (1H, m, NH), 12.40 (1H, s, NH); ^{13}C NMR (75 MHz, DMSO-d_6) δ 40.9 (CH_2), 110.5 (CH-pyrrole), 115.7 (d, $J_{C\text{-}F}$ = 21.5 Hz, CH-Ar), 121.8 (2 x CH-Ar), 124.0 (d, $J_{C\text{-}F}$ = 3.2 Hz, CH-Ar), 124.9 (C), 127.6 (C and CH-pyrrole), 128.1 (d, $J_{C\text{-}F}$ = 15.9 Hz, C), 129.2 (d, $J_{C\text{-}F}$ = 3.1 Hz, CH-

Ar), 131.9 (d, $J_{C\text{-}F}$ = 8.2 Hz, CH-Ar), 148.1 (C-Ar), 149.1 (2 x CH-Ar), 158.4 (d, $J_{C\text{-}F}$ = 247.1 Hz, C-F), 159.9 (CON), 185.9 (CO); HRMS (ES^+) calcd for $C_{18}H_{14}FN_3O_2$ $[M+H]^+$ 324.1143, found 324.1146; Anal. calcd for $C_{18}H_{14}FN_3O_2$: C, 66.87%, H, 4.36%, N, 13.00%; found: C, 66.81%, H, 4.34%, N, 12.99%.

4-(3-Fluorobenzoyl)-*N*-(pyridin-4-ylmethyl)-1*H*-pyrrole-2-carboxamide (33) Prepared according to general procedure C using 4-(3-fluorobenzoyl)-1*H*-pyrrole-2-carboxylic acid **21** (100 mg, 0.43 mmol), carbonyl diimidazole (140 mg, 0.86 mmol) and 4-picolylamine (0.11 mL, 1.08 mmol) in THF (3 mL). Purification *via* MPLC (silica; 0-5% MeOH in EtOAc) and recrystallisation from EtOAc/petrol gave **33** as a white solid (105 mg, 76%); R_f 0.19 (EtOAc); mp 195-197 ºC; λ_{max} (EtOH)/nm 290, 141; IR υ_{max}/cm^{-1} 3198, 1610, 1573; ^{1}H NMR (500 MHz, DMSO-d_6) δ 4.48 (2H, d, J = 6.0 Hz, $NHCH_2$), 7.30 (2H, d, J = 6.0 Hz, 2 × H-pyridyl), 7.41 (1H, d, J = 1.5 Hz, H-pyrrole), 7.47-7.50 (2H, m, H-Ar and H-pyrrole), 7.53-7.56 (1H, m, H-Ar), 7.59 (1H, dd, J = 5.5 and 7.9 Hz, H-Ar), 7.63-7.65 (2H, m, 2 × H-Ar), 8.51 (2H, d, J = 6.0 Hz, 2 × H-pyridyl), 8.99 (1H, t, J = 6.0 Hz, $NHCH_2$), 12.43 (1H, s, NH); ^{13}C NMR (75 MHz, DMSO-d_6) δ 41.9, 112.1, 115.1, 115.4, 118.6, 118.9, 123.7, 124.2, 124.9, 127.9, 128.4, 131.0, 141.9, 146.6, 160.8, 162.3, 188.2; ^{19}F NMR (470 MHz, DMSO-d_6) δ -112.3; HRMS calcd. for $C_{18}H_{15}FN_3O_2$ $[M+H]^+$ 324.1143, found 324.1146.

4-(4-Fluorobenzoyl)-*N*-(pyridin-4-ylmethyl)-1*H*-pyrrole-2-carboxamide (34) Prepared according to general procedure C using 4-(4-fluorobenzoyl)-1*H*-pyrrole-2-carboxylic acid **22** (50 mg, 0.2 mmol), carbonyl diimidazole (70 mg, 0.42 mmol) and 4-picolylamine (0.05 mL, 0.53 mmol) in THF (3 mL). Purification *via* MPLC (silica; 0-5% MeOH in EtOAc) gave **34** as a white solid (50 mg, 70%); R_f 0.06 (EtOAc); mp 236-237 ºC; λ_{max} (EtOH)/nm 290, 241; IR υ_{max}/cm^{-1} 3328, 3236, 1645, 1600; ^{1}H NMR (500 MHz, DMSO-d_6) δ 4.48 (2H, d, J = 6.0 Hz, $NHCH_2$), 7.30

(2H, d, J = 6.0 Hz, 2 × H-pyridyl), 7.35-7.39 (2H, m, 2 × H-Ar), 7.40 (1H, d, J = 1.3 Hz, H-pyrrole), 7.47 (1H, d, J = 1.3 Hz, H-pyrrole), 7.87-7.89 (2H, m, 2 × H-Ar), 8.51 (2H, d, J = 6.0 Hz, 2 × H-pyridyl), 8.98 (1H, t, J = 6.0 Hz, N*H*CH_2), 12.48 (1H, s br, NH); ^{13}C NMR (125 MHz, DMSO-d_6) δ 41.1, 111.5, 115.3, 115.5, 122.1, 123.9, 127.5, 127.9, 131.2, 131.3, 135.6, 148.5, 149 5, 160.3, 164.1, 187.9; ^{19}F NMR (470 MHz, DMSO-d_6) δ -108.0; HRMS calcd. for $C_{18}H_{15}N_3FO_2$ $[M+H]^+$ 324.1143, found 324.1140.

4-(2-Chlorobenzoyl)-*N*-(pyridin-4-ylmethyl)-1*H*-pyrrole-2-carboxamide (35) Prepared according to general procedure C using 4-(2-chlorobenzoyl)-1*H*-pyrrole-2-carboxylic acid **23** (100 mg, 0.40 mmol), carbonyl diimidazole (130 mg, 0.80 mmol) and 4-picolylamine (0.10 mL, 1.00 mmol) in THF (3 mL). Purification *via* MPLC (silica; 0-5% MeOH in EtOAc) and recrystallisation from EtOAc/petrol gave **35** as a white solid (125 mg, 92%); R_f 0.29 (EtOAc); mp 208-210 ºC; λ_{max} (EtOH)/nm 285, 237; IR υ_{max}/cm^{-1} 3174, 1616, 1568; ^{1}H NMR (500 MHz, DMSO-d_6) δ 4.45 (2H, d, J = 6.0 Hz, NHCH_2), 7.23 (1H, s, H-pyrrole), 7.25 (1H, s, H-pyrrole), 7.28 (1H, d, J = 6.0 Hz, 2 × H-pyridyl), 7.46-7.49 (2H, m, 2 × H-Ar), 7.51-7.55 (1H, m, H-Ar), 7.57 (1H, d, J = 8.0 Hz, H-Ar), 8.51 (2H, d, J = 6.0 Hz, 2 × H-pyridyl), 8.98 (1H, t, J = 6.0 Hz, N*H*CH_2), 12.42 (1H, s br, NH); ^{13}C NMR (75 MHz, DMSO-d_6) δ 41.1, 110.7, 122.1, 124.9, 127.1, 128.0, 128.4, 128.5, 129.4, 129.8, 131.0, 139.5, 148.5, 149.5, 160.2, 188.4; HRMS calcd. for $C_{18}H_{15}N_3O_2{}^{35}Cl$ $[M+H]^+$ 340.0847, found 340.0842.

4-(3-Chlorobenzoyl)-*N*-(pyridin-4-ylmethyl)-1*H*-pyrrole-2-carboxamide (36) Prepared according to general procedure C using 4-(3-chlorobenzoyl)-1*H*-pyrrole-2-carboxylic acid **24** (100 mg, 0.40 mmol), carbonyl diimidazole (130 mg, 0.80 mmol) and 4-picolylamine (0.10 mL, 1.0 mmol) in THF (3 mL). Purification *via* MPLC (silica; 0-80% EtOAc in petroleum ether) gave **36** as a white solid (125 mg, 90%); R_f 0.17 (10% MeOH in EtOAc); mp 192-194 ºC; λ_{max} (EtOH)/nm

299, 243; IR υ_{max}/cm^{-1} 3196, 1608, 1569; ^{1}H NMR (500 MHz, DMSO-d_6) δ 4.49 (2H, d, J = 6.0 Hz, NHCH_2), 7.31 (2H, d, J = 6.0 Hz, 2 × H-pyridyl), 7.41 (1H, s, H-pyrrole), 7.50 (1H, s, H-pyrrole), 7.58 (1H, dd, J = 7.8 and 8.0 Hz, H-Ar), 7.69-7.71 (1H, m, H-Ar), 7.74-7.76 (2H, m, 2 × H-Ar), 8.52 (2H, d, J = 6.0 Hz, 2 × H-pyridyl), 9.01 (1H, t, J = 6.0 Hz, NHCH$_2$), 12.45 (1H, s br, NH); ^{13}C NMR (75 MHz, DMSO-d_6) δ 41.1, 111.4, 122.1, 123.6, 127.2, 127.7, 127.9, 128.2, 130.5, 131.4, 133.3, 141.1, 148.5, 149.5, 160.3, 187.8; HRMS calcd. for $C_{18}H_{15}{}^{35}ClN_3O_2$ $[M+H]^+$ 340.0847, found 340.0851.

4-(4-Chlorobenzoyl)-*N*-(pyridin-4-ylmethyl)-1*H*-pyrrole-2-carboxamide (37) Prepared according to general procedure C using 4-(4-chlorobenzoyl)-1*H*-pyrrole-2-carboxylic acid **25** (100 mg, 0.40 mmol), carbonyl diimidazole (130 mg, 0.80 mmol) and 4-picolylamine (0.10 mL, 1.00 mmol) in THF (3 mL). Purification *via* MPLC (silica; 0-5% MeOH in EtOAc) and recrystallisation from EtOAc/petrol gave **37** as a white solid (110 mg, 80%); R_f 0.13 (EtOAc); mp 213-215 ºC; λ_{max} (EtOH)/nm 290, 246; IR υ_{max}/cm^{-1} 3350, 1628, 1568; ^{1}H NMR (500 MHz, DMSO-d_6) δ 4.48 (2H, d, J = 6.0 Hz, NHCH_2), 7.30 (2H, d, J = 6.0 Hz, 2 × H-pyridyl), 7.39 (1H, d, J = 1.5 Hz, H-pyrrole), 7.48 (1H, d, J = 1.5 Hz, H-pyrrole), 7.60 (2H, d, J = 7.5 Hz, 2 × H-Ar), 7.81 (2H, d, J = 7.5 Hz, 2 × H-Ar), 8.51 (2H, d, J = 6.0 Hz, 2 × H-pyridyl), 8.98 (1H, t, J = 6.0 Hz, CH$_2$NH); ^{13}C NMR (75 MHz, DMSO-d_6) δ 41.1, 111.4, 122.1, 123.8, 127.6, 128.0, 128.6, 130.4, 136.5, 137.8, 148.5, 149.5, 160.3, 188.1; HRMS calcd. for $C_{18}H_{15}N_3O_2{}^{35}Cl$ $[M+H]^+$ 340.0847, found 340.0849.

4-(2,3-Difluorobenzoyl)-*N*-(pyridin-4-ylmethyl)-1*H*-pyrrole-2-carboxamide (38) Prepared according to general procedure C using 4-(2,3-difluorobenzoyl)-1*H*-pyrrole-2-carboxylic acid **26** (100 mg, 0.40 mmol), carbonyl diimidazole (130 mg, 0.80 mmol) and 4-picolylamine (0.10 mL, 1.0 mmol) in THF (3 mL). Purification *via* MPLC (silica; 0-5% MeOH in EtOAc) and recrystallisation from EtOAc/petrol gave **38** as a white solid (110 mg, 81%); R_f 0.20 (EtOAc); mp

244-246 ºC; λ_{max} (EtOH)/nm 287, 238; IR υ_{max}/cm^{-1} 3121, 1627, 1568; ^{1}H NMR (300 MHz, DMSO-d_6) δ 4.48 (2H, d, J = 6.0 Hz, NHCH_2), 7.30 (2H, d, J = 6.0 Hz, 2 × H-pyridyl), 7.34 (1H, s, H-pyrrole), 7.35-7.39 (2H, m, 2 × H-Ar), 7.44 (1H, s, H-pyrrole), 7.60-7.66 (1H, m, H-Ar), 8.51 (2H, d, J = 6.0 Hz, 2 × H-pyridyl), 8.97 (1H, t, J = 6.0 Hz, NHCH$_2$), 12.47 (1H, s br, NH); ^{13}C NMR (75 MHz, DMSO-d_6) δ 41.7, 111.2, 119.5, 122.6, 125.0, 125.3, 125.5, 128.6, 128.9, 130.9, 146.9, 148.8, 148.9, 150.4, 160.6, 185.2; ^{19}F NMR (470 MHz, DMSO-d_6) δ -137.8, -141.5; HRMS calcd. for $C_{18}H_{14}F_2N_3O_2$ $[M+H]^+$ 342.1049, found 342.1050.

4-(2,6-Difluorobenzoyl)-*N*-(pyridin-4-ylmethyl)-1*H*-pyrrole-2-carboxamide (39) Prepared according to general procedure C using 4-(2,6-difluorobenzoyl)-1*H*-pyrrole-2-carboxylic acid **27** (50 mg, 0.2 mmol), carbonyl diimidazole (65 mg, 0.4 mmol) and 4-picolylamine (0.05 mL, 0.5 mmol) in THF (3 mL). Purification *via* MPLC (silica; 0-95% EtOAc in petroleum ether) and recrystallisation from EtOAc/petrol gave **39** as a white solid (50 mg, 73%); R_f 0.19 (EtOAc); mp 226-227 ºC; λ_{max} (EtOH)/nm 284, 236; IR υ_{max}/cm^{-1} 3265, 2921, 1624; ^{1}H NMR (500 MHz, DMSO-d_6) δ 4.46 (2H, d, J = 6.0 Hz, NHCH_2), 7.24-7.27 (2H, m, 2 × H-Ar), 7.29-7.30 (3H, m, H-pyrrole, 2 × H-pyridyl), 7.43 (1H, s, H-pyrrole), 7.58-7.64 (1H, m, H-Ar), 8.51 (2H, d, J = 6.0 Hz, 2 × H-pyridyl), 8.97 (1H, t, J = 6.0 Hz, NHCH$_2$), 12.53 (1H, s br, NH); ^{13}C NMR (125 MHz, DMSO-d_6) δ 41.1, 110.3, 112.3, 117.9, 122.1, 125.7, 128.3, 128.5, 132.1, 148.4, 149.5, 158.6, 160.1, 181.8; ^{19}F NMR (470 MHz, DMSO-d_6) δ -114.3; HRMS calcd. for $C_{18}H_{14}F_2N_3O_2$ $[M+H]^+$ 342.1049, found 342.1048.

4-(2,6-Dichlorobenzoyl)-*N*-(pyridin-4-ylmethyl)-1*H*-pyrrole-2-carboxamide (40) Prepared according to general procedure C using 4-(2,6-dichlorobenzoyl)-1*H*-pyrrole-2-carboxylic acid **28** (100 mg, 0.35 mmol), carbonyl diimidazole (115 mg, 0.70 mmol) and 4-picolylamine (0.09 mL, 0.88 mmol) in THF (3 mL). Purification *via* MPLC (silica; 0-5% MeOH in EtOAc) and

recrystallisation from EtOAc/petrol gave **40** as a white solid (110 mg, 84%); R_f 0.31 (EtOAc); mp 143-145 ºC; λ_{max} (EtOH)/nm 285, 237, 206; IR υ_{max}/cm^{-1} 1628, 1559; ^{1}H NMR (500 MHz, DMSO-d_6) δ 4.45 (2H, d, *J* = 6.0 Hz, NHC*H*$_2$), 7.22 (1H, s, H-pyrrole), 7.29 (2H, d, *J* = 6.0 Hz, 2 × H-pyridyl), 7.32 (1H, s, H-pyrrole), 7.52 (1H, dd, *J* = 7.0 and 7.1 Hz, H-Ar), 7.58-7.60 (2H, m, 2 × H-Ar), 8.50 (2H, d, *J* = 6.0 Hz, 2 × H-pyridyl), 8.98 (1H, t, *J* = 6.0 Hz, N*H*CH$_2$), 12.49 (1H, s br, NH); ^{13}C NMR (125 MHz, DMSO-d_6) δ 41.1, 110.2, 122.1, 124.3, 128.3, 128.4, 128.5, 130.5, 131.3, 138.3, 148.4, 149.5, 160.1, 185.8; HRMS calcd. for $C_{18}H_{14}{}^{35}Cl_2N_3O_2$ $[M+H]^+$ 374.0458, found 374.0462.

4-(2,6-Difluorobenzoyl)-*N*-(pyridin-4-yl)-1*H*-pyrrole-2-carboxamide (41) Prepared according to general procedure C using 4-(2,6-difluorobenzoyl)-1*H*-pyrrole-2-carboxylic acid **27** (100 mg, 0.40 mmol), carbonyl diimdazole (129 mg, 0.80 mmol), 4-aminopyridine (94 mg, 1.00 mmol) and THF (4 mL). Purification *via* MPLC (silica; 2-30% MeOH in EtOAc) gave **41** as a white solid (50 mg, 38%); R_f = 0.52 (5% MeOH in EtOAc); mp degraded >290 °C; λ_{max} (EtOH)/nm: 292, 271; υ_{max}/cm^{-1}: 3655, 3368, 2585, 2235, 2019, 1588, 1506; ^{1}H NMR (500 MHz, DMSO-d_6) δ 7.26-7.30 (2H, m, H-3' and H-5'); 7.57 (1H, s, H-3), 7.58 (1H, s, H-5), 7.64 (1H, dddd, *J* = 6.7, 6.8, 8.4 and 8.5 Hz, H-4'), 7.75 (2H, d, *J* = 6.4 Hz, CH-pyridine), 8.47 (2H, d, *J* = 6.4 Hz, CH-N-pyridine), 10.36 (1H, s, CONH), 12.78 (1H, br s, NH); ^{13}C NMR (125 MHz, MeOD) δ 112.1 (C-Ar), 112.2 (C-Ar), 112.4 (C-Ar), 113.7 (C-Ar), 122.0 (C-3), 125.9 (C-2 and C-5), 129.9 (C-4), 145.6 (C-Ar), 150.3 (C-Ar), 157.7 (C-Ar), 159.6 (C-Ar) 159.7 (CONH), 181.8 (CO); ^{19}F NMR (470 MHz, MeOD) δ -114.1; MS (ES$^+$) *m/z* 328.10 $[M+H]^+$; HRMS *m/z* calcd for $C_{17}H_{12}F_2N_3O_2$ $[M+H]^+$ 328.0890, found 328.0890.

4-(2,6-Difluorobenzoyl)-*N*-(pyridin-3-yl)-1*H*-pyrrole-2-carboxamide (42) Prepared according to general procedure C using 4-(2,6-difluorobenzoyl)-1*H*-pyrrole-2-carboxylic acid **27** (50 mg,

0.20 mmol), carbonyldiimidazole (65 mg, 0.40 mmol), 3-aminopyridine (47 mg, 0.50 mmol) and THF (2 mL). Purification *via* MPLC (silica; 0-30% MeOH in EtOAc) **42** as a white solid (23 mg, 35%); R_f 0.78 (5% MeOH in EtOAc); mp 160-161 °C; λ_{max} (EtOH)/nm 290, 240; IR υ_{max}/cm^{-1} 3243, 3021, 2437, 1622, 1538; ^{1}H NMR (500 MHz, DMSO-d_6) δ 7.04-7.07 (2H, m, H-3' and H-5'), 7.15 – 7.17 (1H, m, H-3), 7.30-7.32 (2H, m, CH-pyridine), 7.41 (1H, dddd, J = 6.8, 6.8, 8.5 and 8.5 Hz, H-4'), 7.90-7.93 (1H, m, H-5), 8.08 (1H, dd, J = 1.5 and 4.7 Hz, CH-pyridine), 8.67 (1H, d, J = 2.5 Hz CH-N-pyridine), 10.02 (1H, s, CONH), 12.50 (1H, s br, NH); ^{13}C NMR (125 MHz, MeOD) δ 112.9, 113.1, 122.6, 125.2, 128.0, 129.5, 130.6, 133.2, 136.4, 137.5, 142.4, 145.1, 160.9, 184.7; ^{19}F NMR (470 MHz, MeOD) δ -115.4; HRMS calcd for $C_{17}H_{12}F_2N_3O_2$ $[M+H]^+$ 328.0894, found 328.0895.

4-(2-Chloro-6-fluorobenzoyl)-*N*-(pyridin-4-yl)-1*H*-pyrrole-2-carboxamide (43) Prepared according to general procedure D using 4-(2-chloro-6-fluorobenzoyl)-1*H*-pyrrole-2-carboxylic acid **29** (75 mg, 0.28 mmol), MeCN (1.5 mL), 4-aminopyridine (66 mg, 0.70 mmol) and PCl_3 (25 µL, 0.28 mmol). Purification *via* MPLC (silica; 0-8% MeOH in DCM) gave **43** as a white solid (59 mg, 61%); R_f 0.31 (5% MeOH in DCM); mp degraded >270 °C; λ_{max} (EtOH)/nm 341, 291, 271; IR υ_{max}/cm^{-1} 3416, 3354, 1682, 1632, 1586, 1552, 1506; ^{1}H NMR (500 MHz, DMSO-d_6) δ 7.40-7.43 (1H, m, H-5'), 7.47-7.48 (1H, m, H-3'), 7.51 (1H, s, H-3), 7.55 (1H, s, H-5), 7.59 (1H, ddd, J = 6.2, 8.3 and 8.4 Hz, H-4'), 7.74 (2H, d, J = 6.3 Hz, CH-pyridine), 8.47 (2H, d, J = 6.3 Hz, N-CH-pyridine), 10.36 (1H, s, CO-NH), 12.76 (1H, s, NH); ^{13}C NMR (125 MHz, DMSO-d_6) δ 112.1, 113.7, 115.0, 125.3, 125.9, 127.9, 128.0, 129.8, 130.4, 131.9, 145.6, 150.3, 158.6, 159.0, 183.9; HRMS calcd for $C_{17}H_{11}{}^{35}ClFN_3O_2$ $[M+H]^+$ 344.0597, found 344.0592.

4-(2-Chloro-6-fluorobenzoyl)-*N*-(pyridin-3-yl)-1*H*-pyrrole-2-carboxamide (44) Prepared according to general procedure D using 4-(2-chloro-6-fluorobenzoyl)-1*H*-pyrrole-2-carboxylic

acid **29** (75 mg, 0.28 mmol), MeCN (1.5 mL), 3-aminopyridine (66 mg, 0.70 mmol) and PCl_3 (25 µL, 0.28 mmol). Purification *via* MPLC (silica; 0-8% MeOH in DCM) gave **44** as a white solid (62 mg, 64%); R_f 0.29 (5% MeOH in DCM); mp degraded >260 °C; λ_{max} (EtOH)/nm 350, 248; IR υ_{max}/cm^{-1} 3122, 2963, 1635, 1602, 1535; ^{1}H NMR (500 MHz, DMSO-d_6) δ 7.38-7.43 (2H, m, H-3 and H-5'), 7.47-7.50 (3H, m, H-5, H-3' and CH-pyridine), 7.59 (1H, ddd, *J* = 6.2, 8.3 and 8.4 Hz, H-4'), 8.14 (1H, ddd, *J* = 1.5, 2.5 and 8.3 Hz, CH-pyridine), 8.30 (1H, dd, *J* = 1.5 and 4.7 Hz, N-CH-pyridine), 8.89 (1H, d, *J* = 2.5 Hz, N-CH-pyridine), 10.24 (1H, s, CO-NH), 12.71 (1H, s, NH); ^{13}C NMR (125 MHz, DMSO-d_6) δ 111.6, 115.0, 123.5, 125.3, 125.9, 127.0, 128.0, 128.2, 129.3, 130.4, 131.8, 135.5, 141.6, 144.4, 158.6, 158.7, 183.9; HRMS calcd for $C_{17}H_{11}{}^{35}ClFN_3O_2$ $[M+H]^+$ 344.0597, found 344.0592.

4-(2-Bromo-6-fluorobenzoyl)-*N*-(pyridin-4-yl)-1*H*-pyrrole-2-carboxamide (45) Prepared according to general procedure D using 4-(2-bromo-6-fluorobenzoyl)-1*H*-pyrrole-2-carboxylic acid **30** (50 mg, 0.16 mmol), MeCN (1 mL), 4-aminopyridine (38 mg, 0.40 mmol) and PCl_3 (14 µL, 0.16 mmol). Purification *via* MPLC (silica; 0-8% MeOH in DCM) gave **45** as a white solid (52 mg, 84%); R_f 0.32 (5% MeOH in DCM); mp degraded >150 °C; λ_{max} (EtOH)/nm 291, 270; IR υ_{max}/cm^{-1} 3344, 3112, 2958, 1627, 1591, 1557, 1506; ^{1}H NMR (500 MHz, DMSO-*d6*) δ 7.42-7.46 (1H, m, H-5'), 7.49-7.54 (3H, m, H-3, H-4' and H-5), 7.61-7.62 (1H, m, H-3'), 7.73 (2H, d, *J* = 6.4 Hz, CH-pyridine), 8.46 (2H, d, *J* = 6.4 Hz, N-CH-pyridine), 10.35 (1H, s, CONH), 12.74 (1H, s, NH); ^{13}C NMR (125 MHz, DMSO-*d6*) δ 112.1, 113.7, 115.4, 119.0, 125.0, 128.0, 128.9, 129.8, 132.2, 145.6, 150.3, 158.5, 159.0, 184.9; HRMS calcd for $C_{17}H_{11}{}^{79}BrFN_3O_2$ $[M+H]^+$ 388.0091, found 388.0088.

4-(2-Bromo-6-fluorobenzoyl)-*N*-(pyridin-3-yl)-1*H*-pyrrole-2-carboxamide (46) Prepared according to general procedure D using 4-(2-bromo-6-fluorobenzoyl)-1*H*-pyrrole-2-carboxylic

acid **30** (50 mg, 0.16 mmol), MeCN (1 mL), 3-aminopyridine (38 mg, 0.40 mmol) and PCl_3 (14 μL, 0.16 mmol). Purification *via* MPLC (silica; 0-8% MeOH in DCM) gave **46** as a white solid (47 mg, 76%); R_f 0.31 (5% MeOH in DCM); mp 138-140 °C; λ_{max} (EtOH)/nm 288; IR υ_{max}/cm^{-1} 3127, 2960, 1635, 1599, 1534; ^1H NMR (500 MHz, DMSO-d_6) δ 7.39 (1H, dd, J = 4.7 and 8.4 Hz, CH-pyridine), 7.42-7.48 (3H, m, H-3, H-5' and H-5), 7.52 (1H, ddd, J = 6.2, 8.3 and 8.4 Hz, H-4'), 7.61-7.63 (1H, m, H-3'), 8.14 (1H, ddd, J = 1.5, 2.5 and 8.4 Hz, CH-pyridine), 8.30 (1H, dd, J = 1.5 and 4.7 Hz, N-CH-pyridine), 8.89 (1H, d, J = 2.5 Hz, N-CH-pyridine), 10.24 (1H, s, CONH), 12.70 (1H, s, NH); ^{13}C NMR (125 MHz, DMSO-d_6) δ 111.7, 115.4, 119.0, 123.6, 124.9, 127.0, 128.8, 129.4, 130.0, 132.1, 135.5, 141.6, 144.4, 158.5, 158.7, 184.9; HRMS calcd for $C_{17}H_{11}{}^{79}BrFN_3O_2$ $[M+H]^+$ 388.0091, found 388.0090.

ASSOCIATED CONTENT

Supporting Information

Full kinase panel selectivity data for **46** and crystallographic data are available free of charge.

Funding Information

Accession codes

The coordinates for the ERK5-**46** complex has been deposited in the wwPDB under accession number 5O7I. Authors will release the atomic coordinates and experimental data upon article publication.

AUTHOR INFORMATION

Corresponding Author

*E-mail: celine.cano@newcastle.ac.uk. Phone (+44) 191 208 7060.

Author Contributions

Stephanie Myers - Synthesis and characterization of compounds

Lauren Molyneux - Synthesis and characterization of compounds and manuscript preparation

Duncan C. Miller - Synthesis and characterization of compounds and manuscript preparation

Mercedes Arasta - Performed biological assays

Ruth H. Bawn - Synthesis and characterization of compounds

Timothy Blackburn - Synthesis and characterization of compounds

Simon J. Cook - Experimental design and interpretation, data analysis

Noel Edwards - Performed biological assays

Jane A. Endicott - Experimental design and interpretation, data analysis

Bernard T. Golding - Experimental design and interpretation, data analysis

Roger J. Griffin - Experimental design and interpretation, data analysis

Tim Hammonds - Experimental design and interpretation, data analysis

Ian R. Hardcastle - Experimental design and interpretation, data analysis

Suzannah J. Harnor - Synthesis and characterization of compounds

Amy Heptinstall - Synthesis and characterization of compounds and manuscript preparation

Pamela Lochhead - Assay development and performed biological assays

Mathew P. Martin - Protein expression, crystallisation and structure determination, assay development and manuscript preparation

Nick C. Martin - Synthesis and characterization of compounds

David R. Newell - Experimental design and interpretation, data analysis and manuscript preparation

Paul J. Owen – Protein purification

Leon C. Pang – Protein cloning and expression

Tristan Reuillon - Synthesis and characterization of compounds

Laurent J. M. Rigoreau - Experimental design and interpretation, data analysis

Huw Thomas – Performed biological assays

Julie A. Tucker - Protein expression, crystallisation and structure determination, assay development and manuscript preparation

Lan-Zhen Wang – Performed biological assays

Ai-Ching Wong – Performed biological assays

Martin E. M. Noble - Experimental design and interpretation, data analysis and manuscript preparation

Stephen R. Wedge - Experimental design and interpretation and manuscript preparation

Celine Cano - Project conception, experimental design and interpretation, data analysis and manuscript preparation (submitting author)

Notes

There are no conflicts of interest to declare.

ACKNOWLEDGMENTS

The authors thank Cancer Research UK (Grant Reference C2115/A21421) and the Medical Research Council (Grant Reference MR/K007580/1) for financial support. The authors would also like to thank Diamond Light Source for beam time (proposals mx9948-60 and mx13587-7), the staff of beamlines I04 and I24, and Dr. Arnaud Baslé for assistance with crystal testing and data collection. The gene encoding the first bromodomain of human BRD4 was a kind gift from Astex

Pharmaceuticals (Cambridge, UK). The use of the EPSRC UK National Mass Spectrometry Facility at the University of Wales (Swansea) is also gratefully acknowledged.

ABBREVIATIONS USED

ERK5, extracellular regulated kinase 5; MEK, mitogen-activated protein kinase kinase; BRD, bromodomain; CDI, carbonyldiimidazole; ER, efflux ratio; HLM, human liver microsomes; MLM, mouse liver microsomes; MOI, multiplicity of infection;MPLC, medium-pressure liquid chromatography; LC-MS, liquid chromatography–mass spectrometry; IC_{50}, half maximal inhibitory concentration; MEF2D, Myocyte enhancer factor 2; ppb, plasma protein binding.

REFERENCES

[1] G.N. Nithianandarajah-Jones, B. Wilm, C.E. Goldring, J. Muller, M.J. Cross, ERK5: structure, regulation and function, Cell. Signal., 24 (2012) 2187-2196.
[2] G.V. Long, J.-J. Grob, P. Nathan, A. Ribas, C. Robert, D. Schadendorf, S.R. Lane, C. Mak, P. Legenne, K.T. Flaherty, M.A. Davies, Factors predictive of response, disease progression, and overall survival after dabrafenib and trametinib combination treatment: a pooled analysis of individual patient data from randomised trials, Lancet Oncol., 17 (2016) 1743-1754.
[3] B.A. Drew, M.E. Burow, B.S. Beckman, MEK5/ERK5 pathway: the first fifteen years, Biochim. Biophys. Acta, 1825 (2012) 37-48.
[4] P.A. Lochhead, R. Gilley, S.J. Cook, ERK5 and its role in tumour development, Biochem. Soc. Trans., 40 (2012) 251-256.
[5] R.J. Tatake, M.M. O'Neill, C.A. Kennedy, A.L. Wayne, S. Jakes, D. Wu, S.Z. Kugler, M.A. Kashem, P. Kaplita, R.J. Snow, Identification of pharmacological inhibitors of the MEK5/ERK5 pathway, Biochem. Biophys. Res. Commun., 377 (2008) 120-125.
[6] Q. Yang, X. Deng, B. Lu, M. Cameron, C. Fearns, M.P. Patricelli, J.R. Yates, 3rd, N.S. Gray, J.D. Lee, Pharmacological inhibition of BMK1 suppresses tumor growth through promyelocytic leukemia protein, Cancer Cell, 18 (2010) 258-267.
[7] E.C.K. Lin, C.M. Amantea, T.K. Nomanbhoy, H. Weissig, J. Ishiyama, Y. Hu, S. Sidique, B. Li, J.W. Kozarich, J.S. Rosenblum, ERK5 kinase activity is dispensable for cellular immune response and proliferation, Proc. Natl. Acad. Sci. U. S. A., 113 (2016) 11865-11870.
[8] D. Nguyen, C. Lemos, L. Wortmann, K. Eis, S.J. Holton, U. Boemer, D. Moosmayer, U. Eberspaecher, J. Weiske, C. Lechner, S. Prechtl, D. Suelzle, F. Siegel, F. Prinz, R. Lesche, B. Nicke, K. Nowak-Reppel, H. Himmel, D. Mumberg, F. von Nussbaum, C.F. Nising, M. Bauser, A. Haegebarth, Discovery and Characterization of the Potent and Highly Selective (Piperidin-4-

yl)pyrido[3,2-d]pyrimidine Based in vitro Probe BAY-885 for the Kinase ERK5, J. Med. Chem., 62, (2018), 928-940.
[9] Y. Kato, R.I. Tapping, S. Huang, M.H. Watson, R.J. Ulevitch, J.D. Lee, Bmk1/Erk5 is required for cell proliferation induced by epidermal growth factor, Nature, 395 (1998) 713-716.
[10] P.A. Lochhead, J. Clark, L.Z. Wang, L. Gilmour, M. Squires, R. Gilley, C. Foxton, D.R. Newell, S.R. Wedge, S.J. Cook, Tumor cells with KRAS or BRAF mutations or ERK5/MAPK7 amplification are not addicted to ERK5 activity for cell proliferation, Cell Cycle, 15 (2016) 506-518.
[11] C. Sticht, K. Freier, K. Knopfle, C. Flechtenmacher, S. Pungs, C. Hofele, M. Hahn, S. Joos, P. Lichter, Activation of MAP kinase signaling through ERK5 but not ERK1 expression is associated with lymph node metastases in oral squamous cell carcinoma (OSCC), Neoplasia, 10 (2008) 462-470.
[12] A.E. Simoes, D.M. Pereira, S.E. Gomes, H. Brito, T. Carvalho, A. French, R.E. Castro, C.J. Steer, S.N. Thibodeau, C.M. Rodrigues, P.M. Borralho, Aberrant MEK5/ERK5 signalling contributes to human colon cancer progression via NF-kappaB activation, Cell Death Dis., 6 (2015) e1718.
[13] J.C. Montero, A. Ocana, M. Abad, M.J. Ortiz-Ruiz, A. Pandiella, A. Esparis-Ogando, Expression of Erk5 in early stage breast cancer and association with disease free survival identifies this kinase as a potential therapeutic target, PLoS ONE, 4 (2009) e5565.
[14] M. Miranda, E. Rozali, K.K. Khanna, F. Al-Ejeh, MEK5-ERK5 pathway associates with poor survival of breast cancer patients after systemic treatments, Oncoscience, 2 (2015) 99-101.
[15] S.R. McCracken, A. Ramsay, R. Heer, M.E. Mathers, B.L. Jenkins, J. Edwards, C.N. Robson, R. Marquez, P. Cohen, H.Y. Leung, Aberrant expression of extracellular signal-regulated kinase 5 in human prostate cancer, Oncogene, 27 (2008) 2978-2988.
[16] S.M. Kim, H. Lee, Y.S. Park, Y. Lee, S.W. Seo, ERK5 regulates invasiveness of osteosarcoma by inducing MMP-9, J. Orthop. Res., 30 (2012) 1040-1044.
[17] A.K. Ramsay, S.R. McCracken, M. Soofi, J. Fleming, A.X. Yu, I. Ahmad, R. Morland, L. Machesky, C. Nixon, D.R. Edwards, R.K. Nuttall, M. Seywright, R. Marquez, E. Keller, H.Y. Leung, ERK5 signalling in prostate cancer promotes an invasive phenotype, Br. J. Cancer, 104 (2011) 664-672.
[18] M.R. Cronan, K. Nakamura, N.L. Johnson, D.A. Granger, B.D. Cuevas, J.G. Wang, N. Mackman, J.E. Scott, H.G. Dohlman, G.L. Johnson, Defining MAP3 kinases required for MDA-MB-231 cell tumor growth and metastasis, Oncogene, 31 (2012) 3889-3900.
[19] L. Yan, J. Carr, P.R. Ashby, V. Murry-Tait, C. Thompson, J.S. Arthur, Knockout of ERK5 causes multiple defects in placental and embryonic development, BMC Dev. Biol., 3 (2003) 11.
[20] X. Wang, A.J. Merritt, J. Seyfried, C. Guo, E.S. Papadakis, K.G. Finegan, M. Kayahara, J. Dixon, R.P. Boot-Handford, E.J. Cartwright, U. Mayer, C. Tournier, Targeted deletion of mek5 causes early embryonic death and defects in the extracellular signal-regulated kinase 5/myocyte enhancer factor 2 cell survival pathway, Mol. Cell. Biol., 25 (2005) 336-345.
[21] M. Hayashi, S.W. Kim, K. Imanaka-Yoshida, T. Yoshida, E.D. Abel, B. Eliceiri, Y. Yang, R.J. Ulevitch, J.D. Lee, Targeted deletion of BMK1/ERK5 in adult mice perturbs vascular integrity and leads to endothelial failure, J. Clin. Invest., 113 (2004) 1138-1148.
[22] O.L. Roberts, K. Holmes, J. Muller, D.A. Cross, M.J. Cross, ERK5 and the regulation of endothelial cell function, Biochem. Soc. Trans., 37 (2009) 1254-1259.

[23] M. Hayashi, C. Fearns, B. Eliceiri, Y. Yang, J.D. Lee, Big mitogen-activated protein kinase 1/extracellular signal-regulated kinase 5 signaling pathway is essential for tumor-associated angiogenesis, Cancer Res., 65 (2005) 7699-7706.
[24] E.C. Lin, C.M. Amantea, T.K. Nomanbhoy, H. Weissig, J. Ishiyama, Y. Hu, S. Sidique, B. Li, J.W. Kozarich, J.S. Rosenblum, ERK5 kinase activity is dispensable for cellular immune response and proliferation, Proc. Natl. Acad. Sci. U. S. A., 113 (2016) 11865-11870.
[25] M.P. Martin, S.H. Olesen, G.I. Georg, E. Schonbrunn, Cyclin-dependent kinase inhibitor dinaciclib interacts with the acetyl-lysine recognition site of bromodomains, ACS Chem. Biol., 8 (2013) 2360-2365.
[26] S.M. Myers, R.H. Bawn, L.C. Bisset, T.J. Blackburn, B. Cottyn, L. Molyneux, A.-C. Wong, C. Cano, W. Clegg, R.W. Harrington, H. Leung, L. Rigoreau, S. Vidot, B.T. Golding, R.J. Griffin, T. Hammonds, D.R. Newell, I.R. Hardcastle, High-Throughput Screening and Hit Validation of Extracellular-Related Kinase 5 (ERK5) Inhibitors, ACS Comb. Sci., 18 (2016) 444-455.
[27] PAINS liability was assessed by submitting to the online PAINS and aggregator filters http://www.cbligand.org/PAINS (accessed Apr 09, 2018) and http://zinc15.docking.org/patterns/home/ (accessed Apr 09, 2018) .
[28] K. Down, P. Bamborough, C. Alder, A. Campbell, J.A. Christopher, M. Gerelle, S. Ludbrook, D. Mallett, G. Mellor, D.D. Miller, R. Pearson, K. Ray, Y. Solanke, D. Somers, The discovery and initial optimisation of pyrrole-2-carboxamides as inhibitors of p38α MAP kinase, Bioorg. Med. Chem. Lett., 20 (2010) 3936-3940.
[29] T.M. Reuillon, D. C.; Myers, S.; Molyneux, L.; Cano, C.; Hardcastle, I.; Rigoreau, L.; Golding, B.; Noble, M.; Griffin, R., Pyrrolcarboxamide Derivatives for the Inhibition of ERK5, WO2016042341, 2016.
[30] R. Gilley, H.N. March, S.J. Cook, ERK1/2, but not ERK5, is necessary and sufficient for phosphorylation and activation of c-Fos, Cell. Signal., 21 (2009) 969-977.
[31] H. Chen, J. Tucker, X. Wang, P.R. Gavine, C. Phillips, M.A. Augustin, P. Schreiner, S. Steinbacher, M. Preston, D. Ogg, Discovery of a novel allosteric inhibitor-binding site in ERK5: comparison with the canonical kinase hinge ATP-binding site, Acta Crystallogr. D Struct. Biol., 72 (2016) 682-693.
[32] W. Kabsch, Xds, Acta Crystallogr. D Biol. Crystallogr., 66 (2010) 125-132.
[33] M.D. Winn, C.C. Ballard, K.D. Cowtan, E.J. Dodson, P. Emsley, P.R. Evans, R.M. Keegan, E.B. Krissinel, A.G. Leslie, A. McCoy, S.J. McNicholas, G.N. Murshudov, N.S. Pannu, E.A. Potterton, H.R. Powell, R.J. Read, A. Vagin, K.S. Wilson, Overview of the CCP4 suite and current developments, Acta Crystallogr. D Biol. Crystallogr., 67 (2011) 235-242.
[34] C. Vonrhein, C. Flensburg, P. Keller, A. Sharff, O. Smart, W. Paciorek, T. Womack, G. Bricogne, Data processing and analysis with the autoPROC toolbox, Acta Crystallogr. D Biol. Crystallogr., 67 (2011) 293-302.
[35] A. Vagin, A. Teplyakov, Molecular replacement with MOLREP, Acta Crystallogr. D Biol. Crystallogr., 66 (2010) 22-25.
[36] P. Emsley, J.E. Debreczeni, The use of molecular graphics in structure-based drug design, Methods Mol. Biol., 841 (2012) 143-159.
[37] E. Blanc, P. Roversi, C. Vonrhein, C. Flensburg, S.M. Lea, G. Bricogne, Refinement of severely incomplete structures with maximum likelihood in BUSTER-TNT, Acta Crystallogr. D Biol. Crystallogr., 60 (2004) 2210-2221.

[38] C.R. Groom, I.J. Bruno, M.P. Lightfoot, S.C. Ward, The Cambridge Structural Database, Acta Crystallogr. B Struct. Sci. Cryst. Eng. Mater, 72 (2016) 171-179.
[39] I.J. Bruno, J.C. Cole, M. Kessler, J. Luo, W.D. Motherwell, L.H. Purkis, B.R. Smith, R. Taylor, R.I. Cooper, S.E. Harris, A.G. Orpen, Retrieval of crystallographically-derived molecular geometry information, J. Chem. Inf. Comput. Sci., 44 (2004) 2133-2144.

Graphical Abstract

Identification of a Novel Orally Bioavailable ERK5 Inhibitor with Selectivity over p38α and BRD4.

An HTS hit was optimized to give a sub-micromolar ERK5 inhibitor, selective over p38α and BRD4, suitable for use as an *in vivo* tool compound.